Editors' Suggestion

Synthetic and cosmological axion hybridization: Entangled photons, Hanbury Brown–Twiss, and quantum beats

Daniel Boyanovsky *

Department of Physics, University of Pittsburgh, Pittsburgh, Pennsylvania 15260, USA

(Received 6 March 2025; accepted 8 August 2025; published 18 August 2025)

In this article it is argued that synthetic axions, emergent collective excitations in topological insulators or Weyl semimetals, hybridize with the cosmological axion, a compelling dark matter candidate via a common two-photon decay channel since they both couple to electromagnetic fields via a Chern-Simons term. We point out an analogy to a V-type three-level system with the two upper levels identified with the synthetic and cosmological axions decaying into a two-photon state. The Weisskopf-Wigner theory of spontaneous decay in multilevel atoms is complemented and extended to describe the dynamics of hybridization. The final two-photon state features both kinematic and polarization entanglement and displays quantum beats as a consequence of the interference between the decay paths. An initial population of either axion induces a population of the other via hybridization. Consequently, a dark matter axion condensate induces a condensate of the synthetic axion, albeit with small amplitude. We obtain a momentum- and polarization-resolved Hanbury Brown-Twiss (HBT) second-order coherence describing coincident correlated two-photon detection. It exhibits quantum beats with a frequency given by the difference between the energies of the synthetic and cosmological axion and perhaps may be harnessed to detect either type of axion excitations. The case of synthetic axions individually is obtained in the limit of vanishing coupling of the cosmological axion and features similar two-photon correlations. Hence second-order (HBT) two-photon coherence may provide an alternative detection mechanism for emergent condensed matter axionic collective excitations. Similarities and differences with parametrically down converted photons are discussed.

DOI: 10.1103/8bsv-2h9g

I. INTRODUCTION

The axion is a hypothetical elementary particle that was originally introduced in quantum chromodynamics (QCD) as a solution of the strong CP problem [1–3] and is a potentially viable cold dark matter candidate [4–6]. Extensions beyond the standard model of particle physics may include pseudoscalar particles with properties similar to the QCD axion and can also be suitable dark matter candidates [7–10]. While the cosmological axion has not yet been detected, various experiments are focused on its detection [11–14]. An important feature that characterizes the axion field $\phi(\vec{x},t)$ is its pseudoscalar nature and its interaction with photons via pseudoscalar composite operators of gauge fields, such as $\vec{E}\cdot\vec{B}$ in the form of a Chern-Simons term in the Lagrangian density;

$$\mathcal{L}_{CS} = g_a \phi(\vec{x},t)\vec{E}(\vec{x},t)\cdot\vec{B}(\vec{x},t)\,, \tag{1.1}$$

defining the burgeoning field of axion electrodynamics [15].

Remarkably, in condensed matter physics axion quasiparticles emerge as collective excitations in magnetic topological insulators [16–20] or as axionic charge density waves in Weyl semimetals [21–23] or in multilayered metamaterials [24]. These collective excitations couple to electromagnetism via a Chern-Simons term, just as the cosmological axion, leading to topological magnetoelectric effects such as Faraday and Kerr rotations [25–27], with potential impact in axion detection [28]. Whereas there are no experimental confirmations of axionic collective excitations in condensed matter systems yet, recently it has been proposed that the vanishing of the bulk gap at the surface of magnetic topological insulators yield an enhancement of the fluctuations of the axion field near the surface providing a possible platform for their detection [29]. Recent studies [30–32], proposed to exploit the Primakoff effect, axion-photon conversion in presence of an external magnetic field, to probe a condensate of the cosmological dark matter axion with synthetic axion quasiparticle excitations in topological magnetic insulators.

A. Main objectives

Our study is motivated by the observation that the couplings of the synthetic (ϕ_s) and cosmological (ϕ_c) axions to electromagnetism via the Chern-Simons term (1.1) entails that both types emit and absorb two photons, and as a consequence of this common channel they hybridize via the process $\phi_s \Leftrightarrow 2\gamma \Leftrightarrow \phi_c$. Secondly, we realize that there is a compelling analogy to a V-type three level system [33,34] with the upper two levels decaying into a lower state by

*Contact author: boyan@pitt.edu

Published by the American Physical Society under the terms of the Creative Commons Attribution 4.0 International license. Further distribution of this work must maintain attribution to the author(s) and the published article's title, journal citation, and DOI.

spontaneous emission. In this case, if an initial state is prepared in a coherent superposition of the two upper levels, the final state exhibits quantum beats as a consequence of the path interference in the emission process [33,34]. The analogy with synthetic/cosmological axions emerges when the upper two levels are identified with these excitations and the decay is via a two-photon process. The nature of the Chern-Simons coupling suggests that the two-photon final state is entangled both in momentum and polarization. Consequently, the analogy to a V-type system leads us to conclude that the amplitude of the final correlated two-photon state, will exhibit quantum beats with potentially interesting observational consequences. The correlations in the final two-photon state can be revealed by the Hanbury Brown-Twiss (HBT) second-order coherence including polarizations, which should exhibit quantum beat phenomena and may provide an experimentally accessible platform to confirm the hybridization between the synthetic and cosmological axions via coincident photon detection.

We emphasize that the hybridization and dynamical phenomena that our study focuses on are entirely different from the synthetic-cosmological axion coupling via axion-photon conversion in presence of external magnetic fields (Primakoff effect) invoked in Refs. [30–32]. The hybridization phenomena that we study is independent of any external magnetic field. It is a direct consequence of a common two-photon decay channel of synthetic and cosmological axion (quasi)particle excitations, which leads to an off-diagonal one-loop self-energy matrix determined by the two-photon intermediate state.

Our objectives with this study are the following: (i) to study the dynamics of synthetic-cosmological axion hybridization by exploiting the analogy to a V-type three-level system. For this purpose we extend and complement the formulation of references [34–36] of spontaneous emission in multilevel atoms to the quantum field theory of synthetic and cosmological axions. (ii) Using this framework we obtain the amplitude of the two-photon final state resulting from the decay of the respective axion fields, focusing on extracting quantum beat phenomena that results from the interference of the decay channels. (iii) Decay kinematics from the Chern-Simons interaction term determines that this two-photon final state will be entangled both in momentum and in polarization as a consequence of the pseudoscalar nature of the coupling. We introduce a momentum and polarization resolved Hanbury Brown-Twiss (HBT) second-order (intensity) coherence to study two-photon correlations including polarization. (iv) Finally, we recognize a striking analogy to parametric down conversion, suggesting that intensity interferometry (HBT) is also a useful probe of correlations in the case of axions, in particular providing a possible alternative probe of axions in condensed matter platforms.

B. Brief summary of results

(i) We recognize that the coupling of synthetic and cosmological axions to electromagnetism via a Chern-Simons term implies a common two-photon decay channel, which implies hybridization between the two species via the mutual absorption and emission of photons as intermediate states: synthetic axion $\Leftrightarrow 2\gamma \Leftrightarrow$ cosmological axion. This process implies an off-diagonal self-energy.

(ii) A similarity with a V-type three-level atom is established, with the two upper levels identified with the synthetic and cosmological axions, respectively, decaying to a ground level via two-photon spontaneous emission. The Weisskopf-Wigner theory of spontaneous emission in multilevel atoms is adapted to study the dynamics of hybridization and to obtain the amplitude of the two-photon state. The kinematics of decay and the pseudoscalar nature of the Chern-Simons couplings entail that the photons are entangled both in momentum and polarization with a distinct polarization pattern. We obtain the amplitude of this two-photon state to leading order in the couplings. As a direct consequence of hybridization, it is found that if the initial amplitude of one of the axion fields vanishes, the other axion field generates a nonvanishing amplitude during the time evolution. As a corollary, a condensate of the cosmological axion as a dark matter component, induces a condensate of the synthetic axion, albeit with small amplitude determined by the couplings.

(iii) To probe both momentum and polarization entanglement as a telltale signal of axion hybridization, we introduce a momentum- and polarization-resolved Hanbury Brown-Twiss (HBT) second-order coherence (or cross correlation) as a possible experimental tool to study the telltale photon correlations via coincident two-photon detection. It features quantum beats as a consequence of the interference between the decay paths with a beat frequency determined by the difference of the (renormalized) synthetic and cosmological axion single-particle energies.

(iv) We argue that the same HBT correlations may be useful to probe condensed matter axions only, even when the small coupling of the cosmological axion to electromagnetism entails unobservable quantum beat phenomena. By taking the limit of vanishing cosmological axion coupling, it follows that the axion collective excitations in topological insulators and or Weyl semimetals may also be probed via the momentum- and polarization-resolved HBT second-order coherence because the photons from the synthetic axion decay feature the same type of correlations, determined by their coupling to electromagnetism. Therefore, we propose that HBT second-order correlations may be a useful tool to probe synthetic axions.

(v) We recognize a striking similarity to the case of parametrically down-converted photons discussing similarities and differences. This similarity suggests that experimental interferometric methods to study parametric down conversion may also be suitable to study emergent axionic excitations in condensed matter system via their two-photon decay channel with distinct momentum and polarization correlations.

In Sec. II we introduce the effective field theory for synthetic and cosmological axions, and discuss the interaction picture to study time evolution to leading order in the couplings. Section III presents the extension of Weisskopf-Wigner theory that describes the dynamics of spontaneous emission in multilevel atoms to study the nonequilibrium dynamics of hybridization and to obtain the amplitude of the two-photon final state. In Sec. IV the general results are applied to the case of synthetic and cosmological axion hybridization, establishing momentum and polarization entanglement and that interference between the decay paths

leads to quantum beats in the probability amplitude of the two photon state. In this section we introduce the momentum- and polarization-resolved HBT second-order coherence (or cross correlation) as a useful experimental probe to study hybridization via coincident photodetection. Momentum and polarization entanglement with a particular polarization pattern is a telltale sign of axion electrodynamics and HBT correlations may be important useful probes both in the case of hybridization or solely for condensed matter axion excitations as discussed in detail in Sec. V. In this section we also discuss the striking similarity to parametric down conversion suggesting that (HBT) interferometry could also be a useful probe to study axion physics in condensed matter systems.

In Sec. VI we discuss various aspects and caveats of the approximations involved in the analysis. Our conclusions and further avenues of study are summarized in Sec. VII. Various appendixes are devoted to technical aspects.

II. SYNTHETIC AND COSMIC AXIONS

The effective action for the emergent (synthetic) dynamical axion field in topological insulators is given by [17–19][1]

$$S_s = \int d^3x dt \left\{ \frac{1}{2}(\vec{E}^2 - \vec{B}^2) + \frac{\mathcal{J}}{2}\left(\left(\frac{\partial \delta\theta}{\partial t}\right)^2 - (\vec{v}\cdot\vec{\nabla}\delta\theta)^2 - m_s^2\,\delta\theta^{\,2}\right) + \frac{\alpha}{\pi}\,\delta\theta\,\vec{E}\cdot\vec{B}\right\}, \tag{2.1}$$

where the synthetic dynamical axion field $\delta\theta$ is related to the fluctuations of the Neel order parameter in the case of topological magnetic insulators, $\mathcal{J}, \vec{v}$ are model- and material-dependent constants, m_s is the synthetic axion mass [17–19], and α is the fine structure constant. Redefining the (canonically normalized) synthetic axion field

$$\phi_s(\vec{x},t) = \sqrt{\mathcal{J}}\,\delta\theta(\vec{x},t)\,, \tag{2.2}$$

the effective action for the synthetic axion field and the electromagnetic field is

$$S_s = \int d^3x dt \left\{ \frac{1}{2}(\vec{E}^2 - \vec{B}^2) + \frac{1}{2}\left(\left(\frac{\partial \phi_s(\vec{x},t)}{\partial t}\right)^2 - (\vec{v}\cdot\vec{\nabla}\phi_s(\vec{x},t))^2 - m_s^2\,\phi_s^2(\vec{x},t)\right) + g_s\,\phi_s(\vec{x},t)\,\vec{E}\cdot\vec{B}\right\}, \tag{2.3}$$

with $g_s \equiv \alpha/\pi\sqrt{\mathcal{J}}$. While the form of the second bracket in S_s may differ in the realizations of synthetic dynamical axions in topological insulators and Weyl semimetals, the coupling to electromagnetism via the last, Chern-Simons, term is a generic and distinct hallmark of the coupling of synthetic axions to the $U(1)$ gauge fields.

[1]We have absorbed the vacuum dielectric constant, vacuum permittivity and a factor 4π into a redefinition of the gauge fields and set the speed of light $c = 1$.

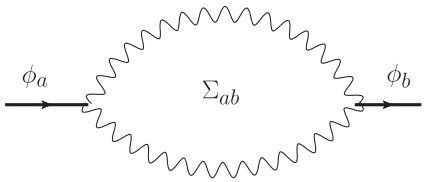


FIG. 1. Synthetic (s) and cosmological (c) axion hybridization via the off-diagonal one loop self-energy diagram with two-photon exchange arising from the correlation function of the Chern-Simons density $\vec{E}\cdot\vec{B}$. The labels $a, b = s, c$.

The effective action for the cosmological axion field $\phi_c(\vec{x},t)$ interacting with electromagnetism is given by [1–3,15]

$$S_c = \int d^3x dt \left\{ \frac{1}{2}(\vec{E}^2 - \vec{B}^2) + \frac{1}{2}\left(\left(\frac{\partial \phi_c(\vec{x},t)}{\partial t}\right)^2 - (\vec{\nabla}\phi_c(\vec{x},t))^2 - m_c^2\,\phi_c^2(\vec{x},t)\right) + g_c\,\phi_c(\vec{x},t)\,\vec{E}\cdot\vec{B}\right\}. \tag{2.4}$$

Therefore we consider the total action that describes together the synthetic and cosmological axions

$$S_{\rm tot} = S_{0\rm EM} + S_{0s} + S_{0c} + \int d^3x dt\,(g_s\phi_s(\vec{x},t) + g_c\phi_c(\vec{x},t)) \times \vec{E}(\vec{x},t)\cdot\vec{B}(\vec{x},t)\,, \tag{2.5}$$

with $S_{0\rm EM}, S_{0s}, S_{0c}$ are the free-field actions for electromagnetism, synthetic, and cosmological axions, respectively. Writing the total action in this form makes manifest that the interactions of the synthetic and cosmological axions with the electromagnetic fields lead to emission/absorption processes $\phi_a \Leftrightarrow 2\gamma \Leftrightarrow \phi_b$ with a two-photon intermediate state and $a, b \equiv s, c$. These processes define the one-loop self-energy matrix $\Sigma_{ab}, a, b = s, c$ depicted in Fig. 1 from which the off-diagonal elements Σ_{sc}, Σ_{cs} describe the mixing or hybridization of the synthetic and cosmological axions.

One of our main objectives is to derive the self-energy matrix and to study the dynamics of hybridization.

The time evolution is determined by the quantum Hamiltonian operator. Since the interaction involves derivative terms, Hamiltonian quantization is subtle because the Chern-Simons interaction modifies the canonical momentum of the gauge field. The proper quantization procedure along with the interaction picture representation are discussed in detail in Appendix A. The main result is that to leading order in the interaction the total Hamiltonian is

$$H = H_{0\rm EM} + H_{0s} + H_{0c} + H_I\,, \tag{2.6}$$

where $H_{0\rm EM}, H_{0s}, H_{0c}$ are the free-field Hamiltonians for electromagnetism, synthetic, and cosmological axions, respectively, and to leading order in the couplings g_s, g_c the interaction Hamiltonian in interaction picture is given by

$$H_I(t) = -\int d^3x (g_s\phi(\vec{x},t) + g_c\phi_c(\vec{x},t))\vec{E}(\vec{x},t)\cdot\vec{B}(\vec{x},t)\,, \tag{2.7}$$

where (see Appendix A)

$$\vec{E}(\vec{x},t) = -\frac{\partial}{\partial t}\vec{A}(\vec{x},t)\,. \tag{2.8}$$

The quantized fields in interaction picture are expanded as

$$\phi_{s,c}(\vec{x},t) = \frac{1}{\sqrt{V}}\sum_{\vec{k}}\frac{1}{\sqrt{2E_{s,c}(k)}}\,[b_{s,c}(\vec{k})\,e^{-iE_{s,c}(k)t}\,e^{i\vec{k}\cdot\vec{x}} + b^{\dagger}_{s,c}(\vec{k})\,e^{iE_{s,c}(k)t}\,e^{-i\vec{k}\cdot\vec{x}}]\,, \tag{2.9}$$

where V is the quantization volume and

$$E_s(k) = \sqrt{(\vec{v}\cdot\vec{k})^2 + m_s^2}, \quad E_c = \sqrt{k^2 + m_c^2}\,, \tag{2.10}$$

are the single (quasi)particle energies for the synthetic (s) and cosmological (c) axions, respectively. In Coulomb gauge the vector potential is given by

$$\vec{A}(\vec{x},t) = \frac{1}{\sqrt{V}}\sum_{\vec{k}}\sum_{\lambda=1,2}\frac{\vec{\epsilon}_{\lambda}(\vec{k})}{\sqrt{2k}}\,[a_{\lambda}(\vec{k})\,e^{-ikt}\,e^{i\vec{k}\cdot\vec{x}} + a^{\dagger}_{\lambda}(\vec{k})\,e^{ikt}\,e^{-i\vec{k}\cdot\vec{x}}]\,, \tag{2.11}$$

where the annihilation and creation operators obey the usual canonical commutation relations and the real linear polarization vectors $\vec{\epsilon}_{\lambda}(\vec{k})$ are defined in Appendix A [see Eq. (A27)].

III. WEISSKOPF-WIGNER THEORY OF HYBRIDIZATION

We begin by extending the formulation of spontaneous emission of multilevel atoms [34–36] based on the Weisskopf-Wigner theory of atomic linewidths [33,34,37], to the case when excitations of different species hybridize via a common set of intermediate states, or common decay channel. The method parallels the effective field theory of flavor-mixing phenomena developed in Ref. [38]. We first discuss the general case, and apply it to the hybridization of synthetic and cosmological axions in the next section.

Consider a system whose Hamiltonian H is given as a soluble part H_0 and a perturbation H_I: $H = H_0 + H_I$. The time evolution of states in the interaction picture of H_0 is given by

$$i\frac{d}{dt}|\Psi(t)\rangle_I = H_I(t)\,|\Psi(t)\rangle_I, \tag{3.1}$$

where the interaction Hamiltonian in the interaction picture is

$$H_I(t) = e^{iH_0 t}H_I e^{-iH_0 t}\,, \tag{3.2}$$

where H_I is proportional to a set of couplings assumed to be small.

The state $|\Psi(t)\rangle_I$ can be expanded as

$$|\Psi(t)\rangle_I = \sum_n C_n(t)|n\rangle, \tag{3.3}$$

where $|n\rangle$ form a complete set of orthonormal states chosen to be eigenfunctions of H_0, namely $H_0|n\rangle = E_n|n\rangle$; in the many body case these are many-particle Fock states. From Eq. (3.1), and the expansion (3.3) one finds the equation of motion for the coefficients $C_n(t)$, namely

$$\dot{C}_n(t) = -i\sum_m C_m(t)\langle n|H_I(t)|m\rangle\,. \tag{3.4}$$

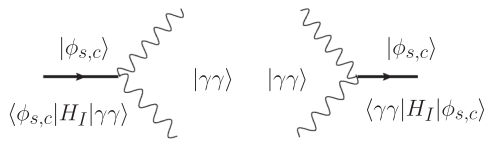


FIG. 2. Hybridization between $|\phi_s\rangle, |\phi_c\rangle$ mediated by a common set of two-photon intermediate states $|\kappa\rangle = |\gamma\gamma\rangle$ with the interaction Hamiltonian $H_I = -\int(g_s\phi_s + g_c\phi_c)\,\vec{E}\cdot\vec{B}\,d^3x$.

Although this equation is exact, it generates an infinite hierarchy of simultaneous equations when the Hilbert space of states spanned by $\{|n\rangle\}$ is infinite dimensional. However, this hierarchy can be truncated by considering the transition between states connected by the interaction Hamiltonian at a given order in H_I.

Let us consider quantum states $|\phi_s\rangle, |\phi_c\rangle$ associated with the synthetic (s) and cosmological (c) axion fields, respectively, these may be single-particle momentum eigenstates of the Fock quanta of these fields, and focus on the case when the interaction Hamiltonian does not couple directly the states $|\phi_s\rangle, |\phi_c\rangle$, namely $\langle\phi_{s,c}|H_I|\phi_{s,c}\rangle = 0$. Instead these states are connected to a common set of intermediate states $|\{\kappa\}\rangle$ by H_I, namely $|\phi_{s,c}\rangle \Rightarrow |\{\kappa\}\rangle \neq |\phi_{s,c}\rangle$. In the case under consideration the states $|\phi_{s,c}\rangle$ are single (quasi)particle excitations of the synthetic and cosmological axion fields, and the intermediate state $|\kappa\rangle$ is a two-photon state created by the operator $\vec{E}\cdot\vec{B}$ as depicted in Fig. 2.

The states $|\phi_s\rangle, |\phi_c\rangle$ hybridize as a consequence of this indirect coupling through the common set of intermediate states, namely $|\phi_{s,c}\rangle \Leftrightarrow |\{\kappa\}\rangle \Leftrightarrow |\phi_{s,c}\rangle$, yielding an off-diagonal self-energy matrix.

In the subspace $|\phi_s\rangle, |\phi_c\rangle, |\{\kappa\}\rangle$ the quantum state in the interaction picture is given by

$$|\Psi\rangle_I(t) = (C_s(t)|\phi_s\rangle + C_c(t)|\phi_c\rangle)\otimes|\{0\}_{\kappa}\rangle + \sum_{\{\kappa\}}C_{\kappa}(t)|\kappa\rangle\otimes|0_s,0_c\rangle\,, \tag{3.5}$$

and the set of equations (3.4) become[2]

$$\dot{C}_s(t) = -i\sum_{\{\kappa\}}\langle\phi_s|H_I(t)|\kappa\rangle\,C_{\kappa}(t) \tag{3.6}$$

$$\dot{C}_c(t) = -i\sum_{\{\kappa\}}\langle\phi_c|H_I(t)|\kappa\rangle\,C_{\kappa}(t)\,, \tag{3.7}$$

$$\dot{C}_{\kappa}(t) = -i[\langle\kappa|H_I(t)|\phi_s\rangle\,C_s(t) + \langle\kappa|H_I(t)|\phi_c\rangle\,C_c(t)]\,. \tag{3.8}$$

where the time-dependent transition matrix elements are given by

$$\langle l|H_I(t)|m\rangle = T_{lm}\,e^{i(E_l-E_m)t}, \quad T_{lm} = \langle l|H_I(0)|m\rangle\,, \tag{3.9}$$

Hermiticity of H_I entails that

$$T_{ml} = T^*_{lm}\,. \tag{3.10}$$

[2]The interaction Hamiltonian also yields contributions in which the initial particle is unaffected and two photons and a synthetic or cosmological axion are produced. These are nonenergy conserving vacuum-type diagrams that will be neglected.

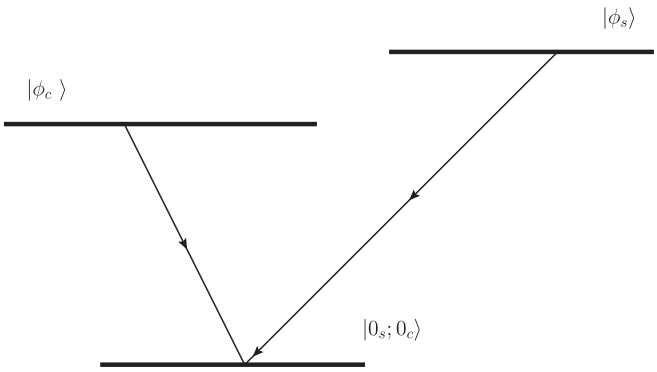


FIG. 3. Equivalence to a V-type atomic system with two upper levels decaying to a common lower level by spontaneous emission.

The set of equations (3.6)–(3.8), truncates the hierarchy of equations by neglecting the transitions between the states $|\{\kappa\}\rangle$ and $|\{\kappa'\}\rangle \neq |\{\kappa\}\rangle$, $|\phi_{1,2}\rangle$, such transitions connect the states $|\phi_{s,c}\rangle \leftrightarrow |\{\kappa'\}\rangle$ at higher order in H_I and are neglected up to $\mathcal{O}(H_I^2)$. Truncating the hierarchy closes the set of equations for the amplitudes, effectively reducing the set of states to a closed subset in the full Hilbert space.

Taking the normalized initial quantum state $|\Psi(t=0)\rangle$ as a coherent linear superposition of the single-particle states $|\phi_{s,c}\rangle$, it is given by

$$|\Psi(t=0)\rangle = (C_s(0)|\phi_s\rangle + C_c(0)|\phi_c\rangle) \otimes |0_\kappa\rangle\,, \tag{3.11}$$

where $|0_\kappa\rangle$ is the vacuum state for the intermediate states $|\kappa\rangle$, in the case under consideration, it corresponds to the electromagnetic vacuum, corresponding to setting

$$C_\kappa(0) = 0\,, \tag{3.12}$$

and with normalization condition

$$|C_s(0)|^2 + |C_c(0)|^2 = 1\,. \tag{3.13}$$

This system is strikingly similar to a V-type system of three atomic levels with the two upper levels decaying to a common lower level by spontaneous emission, depicted in Fig. 3 where the two upper levels are identified with the synthetic and cosmological axion excitations.

This type of systems is ubiquitous in quantum optics [33–36] and gives rise to quantum beats as a consequence of which-path interference.

Unitarity. The set of equations (3.6)–(3.8) describe unitary time evolution in the restricted Hilbert space of states $|\phi_s\rangle, |\phi_c\rangle, |\kappa\rangle$, which is a subset of the full Hilbert space of the theory that is closed under the equations of motion (3.6)–(3.8). Unitarity can be seen as follows: using the equations (3.6)–(3.8), and noticing that $\langle l|H_I(t)|m\rangle^* = \langle m|H_I(t)|l\rangle$ because $H_I(t)$ is an Hermitian operator, it follows from Eqs. (3.6)–(3.8) that

$$\frac{d}{dt}\left[|C_s(t)|^2 + |C_c(t)|^2 + \sum_{\{\kappa\}} |C_\kappa(t)|^2\right] = 0\,, \tag{3.14}$$

and the initial conditions (3.13), (3.12) yield

$$|C_s(t)|^2 + |C_c(t)|^2 + \sum_{\{\kappa\}} |C_\kappa(t)|^2 = 1\,. \tag{3.15}$$

This is the statement that time evolution within the sub-Hilbert space $\{|\phi_s\rangle, |\phi_c\rangle, |\kappa\rangle\}$ is unitary.

In particular if the $\phi_{s,c}$ states decay, it follows that $|C_{s,c}(t=\infty)|^2 = 0$, and asymptotically

$$\sum_\kappa |C_\kappa(t=\infty)|^2 = 1\,. \tag{3.16}$$

The set of equations (3.8) with the initial condition (3.12) can be integrated to yield

$$C_\kappa(t) = -i\int_0^t [T_{\kappa s}\, e^{i(E_\kappa - E_s)t'}\, C_s(t') + T_{\kappa c}\, e^{i(E_\kappa - E_c)t'}\, C_c(t')]\, dt'\,, \tag{3.17}$$

where the labels s, c correspond to $\phi_{s,c}$. Inserting the solution (3.17) into the equations (3.6), (3.7) leads to the following set of equations for the amplitudes $C_s(t), C_c(t)$:

$$\dot{C}_s(t) = -\int_0^t \sum_\kappa \{|T_{s\kappa}|^2\, e^{i(E_s - E_\kappa)(t-t')}\, C_s(t') + T_{s\kappa}T_{\kappa c}\, e^{i(E_1 - E_c)t}\, e^{i(E_c - E_\kappa)(t-t')} C_c(t')\}\, dt'\,, \tag{3.18}$$

$$\dot{C}_c(t) = -\int_0^t \sum_\kappa \{T_{c\kappa}T_{\kappa s}\, e^{i(E_c - E_s)t}\, e^{i(E_s - E_\kappa)(t-t')} C_s(t') + |T_{c\kappa}|^2\, e^{i(E_c - E_\kappa)(t-t')}\, C_c(t')\}\, dt'\,. \tag{3.19}$$

This procedure of solving for the amplitudes of the intermediate states plays the role of tracing over the κ degrees of freedom, yielding an effective set of equations of motion for the amplitudes of the single-particle states $|\phi_{s,c}\rangle$. Since the interaction Hamiltonian H_I is assumed to be proportional to weak couplings, the amplitude equations (3.18), (3.19) are exact up to second order in these couplings.

Markov approximation: Effective non-Hermitian Hamiltonian

Let us define

$$\int_0^{t'} \sum_\kappa T_{a\kappa}T_{\kappa b}\, e^{i(E_b - E_\kappa)(t-t'')}\, dt'' \equiv W_{ab}[t;t'], \quad W_{ab}[t;0] = 0 \tag{3.20}$$

so that

$$\sum_\kappa T_{a\kappa}T_{\kappa b} e^{i(E_b - E_\kappa)(t-t')} = \frac{d}{dt'} W_{ab}[t;t']\,, \tag{3.21}$$

where the labels a, b stand for s (synthetic) or c (cosmological). Inserting this definition in (3.18), (3.19) and integrating by parts

$$\int_0^t \frac{d}{dt'} W_{ab}[t;t']\, C_b(t')\, dt' = W_{ab}[t;t]\, C_b(t) - \int_0^t W_{ab}[t;t']\, \frac{d}{dt'} C_b(t')\, dt'\,, \tag{3.22}$$

since $T_{a\kappa}T_{\kappa b} \propto H_I^2$ and from the evolution equations (3.18), (3.19) it follows that $\dot{C}_a \propto H_I^2$ therefore, the second term on the right-hand side in (3.22) is of $\mathcal{O}(H_I^4)$ and will be neglected to leading order in the interaction, namely H_I^2.

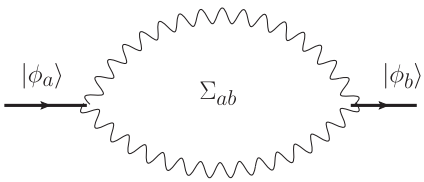


FIG. 4. One loop self-energy diagram corresponding to the two-photon exchange arising from the correlation function of the Chern-Simons density $\vec{E}\cdot\vec{B}$ that hybridizes the synthetic (s) and cosmological (c) axions. The labels $a, b = s, c$.

Hence, up to $\mathcal{O}(H_I^2)$, the evolution equations for the amplitudes (3.18), (3.19) become

$$\dot{C}_s(t) = -\{W_{ss}[t;t]\,C_s(t) + e^{i(E_s-E_c)t}\,W_{sc}[t;t]\,C_c(t)\} \tag{3.23}$$

$$\dot{C}_c(t) = -\{e^{i(E_c-E_s)t}\,W_{cs}[t;t]\,C_s(t) + W_{cc}[t;t]\,C_c(t)\}\,. \tag{3.24}$$

Introducing the Schrödinger picture amplitudes

$$e^{-iE_st}\,C_s(t) \equiv A_s(t), \quad e^{-iE_ct}\,C_c(t) \equiv A_c(t)\,, \tag{3.25}$$

the amplitude equations for $A_{s,c}$ become

$$i\,\dot{A}_s(t) = E_sA_s(t) - i\,W_{ss}[t;t]A_s(t) - i\,W_{sc}[t;t]A_c(t) \tag{3.26}$$

$$i\,\dot{A}_c(t) = E_cA_c(t) - i\,W_{cs}[t;t]A_s(t) - i\,W_{cc}[t;t]A_c(t)\,. \tag{3.27}$$

Following the main Markov approximation in the Weisskopf-Wigner method [33,37] we invoke the long-time limit

$$\int_0^t e^{i(E_b-E_\kappa)(t-t')}\,dt' \underset{t\to\infty}{\longrightarrow} i\left[\mathcal{P}\left(\frac{1}{E_b-E_\kappa}\right) - i\pi\,\delta(E_b-E_\kappa)\right], \tag{3.28}$$

and let us introduce the spectral densities

$$\rho_{ab}(k_0) = \sum_\kappa T_{a\kappa}T_{\kappa b}\,\delta(k_0-E_\kappa) = \rho^*_{ba}(k_0), \quad a,b = s,c\,, \tag{3.29}$$

where the second identity follows from Eq. (3.10), yielding

$$-i\,W_{ab}[t;t] \underset{t\to\infty}{\longrightarrow} \Sigma_{ab}(E_b)\,. \tag{3.30}$$

The self-energy

$$\Sigma_{ab}(E_b) = \int_{-\infty}^{\infty}\frac{\rho_{ab}(k_0)}{E_b-k_0+i\varepsilon}\,dk_0, \quad \varepsilon\to 0^+ \tag{3.31}$$

has a simple and intuitive interpretation as a second order Feynman diagram wherein the lines representing the intermediate states $|\kappa\rangle$ in Fig. 2 are joined into propagators yielding a one loop diagram, representing the self-energy up to second order in H_I. For the case under consideration this Feynman diagram features a two-photon loop arising from the correlation function of the Chern-Simons density $\vec{E}\cdot\vec{B}$ and is depicted in Fig. 4.

This is precisely what was anticipated in Sec. I, confirming the intuitive discussion on hybridization via the common decay channel in Sec. II.

Separating the self-energy into the real and imaginary parts

$$\begin{aligned}\Sigma_{ab}(E_b) &= \Delta_{ab}(E_b) - i\frac{\Gamma_{ab}(E_b)}{2},\\ \Delta_{ab}(E_b) &\equiv \int_{-\infty}^{\infty}\mathcal{P}\left[\frac{\rho_{ab}(k_0)}{E_b-k_0}\right]dk_0,\\ \Gamma_{ab}(E_b) &= 2\pi\,\rho_{ab}(E_b)\,,\end{aligned} \tag{3.32}$$

where $\mathcal{P}$ stands for the principal part. The diagonal components $\Delta_{aa}(E_a)$, $\Gamma_{aa}(E_a)$ are identified as the level shift (Lamb shift) and decay rate (linewidth), respectively, of the synthetic and cosmological axions in absence of hybridization.

Taking this long-time limit, the amplitude equations (3.26), (3.27) become an effective Schrödinger equation with a time-independent effective Hamiltonian

$$i\,\frac{d}{dt}\begin{pmatrix}A_s(t)\\A_c(t)\end{pmatrix} = \mathcal{H}_{\rm eff}\begin{pmatrix}A_s(t)\\A_c(t)\end{pmatrix} \tag{3.33}$$

with

$$\mathcal{H}_{\rm eff} = \begin{pmatrix}E_s+\Sigma_{ss}(E_s) & \Sigma_{sc}(E_c)\\ \Sigma_{cs}(E_s) & E_c+\Sigma_{cc}(E_d)\end{pmatrix} \equiv \begin{pmatrix}\mathcal{H}_{11} & \mathcal{H}_{12}\\ \mathcal{H}_{21} & \mathcal{H}_{22}\end{pmatrix}. \tag{3.34}$$

This effective Hamiltonian is not Hermitian, this is a manifestation that it describes the (approximate) dynamics of a quantum open system, namely of a subset of degrees of freedom, which are coupled to a continuum of other degrees of freedom whose dynamics has been integrated out. Time evolution is not unitary in this subset, as is explicit from the unitarity condition (3.14), (3.15), which indicates a flow of probability from the $|\phi_s\rangle$, $|\phi_c\rangle$ to the excited intermediate states $|\{\kappa\}\rangle$, which have been integrated out in the equations of motion.

It proves convenient to rewrite $\mathcal{H}_{\rm eff}$ as

$$\begin{aligned}\mathcal{H}_{\rm eff} &= \tfrac{1}{2}\,(E_s+\Sigma_{ss}(E_s)+E_c+\Sigma_{cc}(E_c))\,\mathbb{I}\\ &+ \tfrac{1}{2}\,\widetilde{D}(E_s,E_c)\,\widetilde{\mathbb{R}}(E_s,E_c)\,,\end{aligned} \tag{3.35}$$

where $\mathbb{I}$ is the 2×2 identity matrix, $\widetilde{D}(E_s,E_c)$ is given by

$$\begin{aligned}\widetilde{D}(E_s,E_c) = [&(E_s+\Sigma_{ss}(E_s)-E_c-\Sigma_{cc}(E_c))^2\\ &+ 4\,\Sigma_{sc}(E_c)\Sigma_{cs}(E_s)]^{1/2}\,,\end{aligned} \tag{3.36}$$

and

$$\widetilde{\mathbb{R}}(E_s,E_c) = \begin{pmatrix}\widetilde{\alpha}(E_s,E_c) & \widetilde{\beta}(E_s,E_c)\\ \widetilde{\gamma}(E_s,E_c) & -\widetilde{\alpha}(E_s,E_c)\end{pmatrix}, \tag{3.37}$$

with the definitions

$$\widetilde{\alpha}(E_s,E_c) = \frac{(E_s+\Sigma_{ss}(E_s)-E_c-\Sigma_{cc}(E_c))}{\widetilde{D}(E_s,E_c)} \tag{3.38}$$

$$\widetilde{\beta}(E_s,E_c) = \frac{2\,\Sigma_{sc}(E_c)}{\widetilde{D}(E_s,E_c)}\;;\;\widetilde{\gamma}(E_s,E_c) = \frac{2\,\Sigma_{cs}(E_s)}{\widetilde{D}(E_s,E_c)}\,. \tag{3.39}$$

It follows from these definitions that (suppressing the arguments $E_{s,c}$)

$$\widetilde{\alpha}^2 + \widetilde{\beta}\,\widetilde{\gamma} = 1\,, \tag{3.40}$$

which implies that

$$\widetilde{\mathbb{R}}^2(E_s, E_c) = \mathbb{I}\,, \tag{3.41}$$

since $\mathrm{Tr}\,\widetilde{\mathbb{R}} = 0$, the matrix $\widetilde{\mathbb{R}}$ features eigenvalues ± 1.

Consider the eigenvalue equation (suppressing the arguments $E_{s,c}$),

$$\widetilde{\mathbb{R}} \begin{pmatrix} p^{\pm} \\ \pm q^{\pm} \end{pmatrix} = \pm \begin{pmatrix} p^{\pm} \\ q^{\pm} \end{pmatrix}, \tag{3.42}$$

the solution of which is (up to normalization factors)

$$p^{+} = \frac{1}{2}(1+\widetilde{\alpha}), \quad q^{+} = \frac{\widetilde{\gamma}}{2}\,, \tag{3.43}$$

$$p^{-} = -\frac{\widetilde{\beta}}{2}, \quad q^{-} = \frac{1}{2}(1+\widetilde{\alpha})\,. \tag{3.44}$$

From the relation (3.40), we choose

$$\widetilde{\alpha} = \sqrt{1-\widetilde{\beta}\widetilde{\gamma}}\,, \tag{3.45}$$

so that in absence of hybridization, $\widetilde{\beta} = 0; \widetilde{\gamma} = 0$, the eigenvectors are the synthetic and cosmological axion states with eigenvalues ± 1, respectively. The solutions (3.42) are eigenvectors of $\mathcal{H}_{\rm eff}$, namely

$$\mathcal{H}_{\rm eff} \begin{pmatrix} p^{\pm} \\ q^{\pm} \end{pmatrix} = \lambda^{\pm} \begin{pmatrix} p^{\pm} \\ q^{\pm} \end{pmatrix}, \tag{3.46}$$

with eigenvalues

$$\lambda^{\pm} \equiv \widetilde{\varepsilon}^{\pm} - i\,\frac{\widetilde{\Gamma}^{\pm}}{2} = \frac{1}{2}\left[(E_s + \Sigma_{ss}(E_s) + E_2 + \Sigma_{cc}(E_c)) \pm \widetilde{D}(E_s, E_c)\right], \tag{3.47}$$

where $\widetilde{\varepsilon}^{\pm}; \widetilde{\Gamma}^{\pm}$ are both real and defined by Eq. (3.47). These are the energies ($\widetilde{\varepsilon}^{\pm}$) and lifetimes ($\widetilde{\Gamma}^{\pm}$) of the (quasi)normal modes resulting from the hybridization of synthetic and cosmological axions.

The effective Hamiltonian can be diagonalized by introducing

$$U^{-1} = \begin{pmatrix} p^{+} & p^{-} \\ q^{+} & q^{-} \end{pmatrix}; \quad U = \frac{1}{-p^{+}q^{-} + q^{+}p^{-}} \begin{pmatrix} -q^{-} & p^{-} \\ q^{+} & -p^{+} \end{pmatrix}, \tag{3.48}$$

satisfying $UU^{-1} = U^{-1}U = \mathbb{I}$, yielding

$$U\mathcal{H}_{\rm eff}U^{-1} = \begin{pmatrix} \lambda^{+} & 0 \\ 0 & \lambda^{-} \end{pmatrix}. \tag{3.49}$$

Let us define

$$\begin{pmatrix} A_s(t) \\ A_c(t) \end{pmatrix} = U^{-1} \begin{pmatrix} V_s(t) \\ V_c(t) \end{pmatrix}, \tag{3.50}$$

the effective evolution equations for $V_{1,2}(t)$ become

$$i\,\frac{d}{dt}\begin{pmatrix} V_s(t) \\ V_c(t) \end{pmatrix} = \begin{pmatrix} \lambda^{+}V_s(t) \\ \lambda^{-}V_c(t) \end{pmatrix} \Rightarrow \begin{pmatrix} V_s(t) \\ V_c(t) \end{pmatrix} = \begin{pmatrix} e^{-i\lambda^{+}t} & 0 \\ 0 & e^{-i\lambda^{-}t} \end{pmatrix} \begin{pmatrix} V_s(0) \\ V_c(0) \end{pmatrix}. \tag{3.51}$$

Using the definition (3.50) evaluated at $t = 0$ yields the solution for the amplitudes

$$\begin{pmatrix} A_s(t) \\ A_c(t) \end{pmatrix} = U^{-1} \begin{pmatrix} e^{-i\lambda^{+}t} & 0 \\ 0 & e^{-i\lambda^{-}t} \end{pmatrix} U \begin{pmatrix} A_s(0) \\ A_c(0) \end{pmatrix}. \tag{3.52}$$

With the relations (3.40), (3.43), (3.44) it is straightforward to find that

$$\begin{pmatrix} A_s(t) \\ A_c(t) \end{pmatrix} = [e^{-i\lambda^{+}t}\,\widetilde{\mathbb{P}}_{+} + e^{-i\lambda^{-}t}\,\widetilde{\mathbb{P}}_{-}] \begin{pmatrix} A_s(0) \\ A_c(0) \end{pmatrix}, \tag{3.53}$$

with the projector operators

$$\widetilde{\mathbb{P}}_{\pm} = \tfrac{1}{2}(\mathbb{I} \pm \widetilde{\mathbb{R}}), \quad \widetilde{\mathbb{P}}_{\pm}^{2} = \widetilde{\mathbb{P}}_{\pm}\,, \tag{3.54}$$

where $\widetilde{\mathbb{R}}$ is given by Eq. (3.37). These project onto the quasinormal (because of the damping rate) modes. Alternatively

$$\begin{pmatrix} A_s(t) \\ A_c(t) \end{pmatrix} = \frac{1}{2}[(e^{-i\lambda^{+}t} + e^{-i\lambda^{-}t})\,\mathbb{I} + (e^{-i\lambda^{+}t} - e^{-i\lambda^{-}t})\,\widetilde{\mathbb{R}}] \times \begin{pmatrix} A_s(0) \\ A_c(0) \end{pmatrix}. \tag{3.55}$$

Gathering terms, we find

$$A_s(t) = A_s^{(+)}(0)\,e^{-i\varepsilon^{+}t}\;e^{-\frac{\widetilde{\Gamma}^{+}}{2}t} + A_s^{(-)}(0)\,e^{-i\varepsilon^{-}t}\;e^{-\frac{\widetilde{\Gamma}^{-}}{2}t} \tag{3.56}$$

$$A_c(t) = A_c^{(+)}(0)\,e^{-i\varepsilon^{+}t}\;e^{-\frac{\widetilde{\Gamma}^{+}}{2}t} + A_c^{(-)}(0)\,e^{-i\varepsilon^{-}t}\;e^{-\frac{\widetilde{\Gamma}^{-}}{2}t}\,, \tag{3.57}$$

where we used Eq. (3.47), and

$$A_s^{(+)}(0) = \frac{1}{2}\,(1+\widetilde{\alpha})\,A_s(0) + \frac{\widetilde{\beta}}{2}\,A_c(0),$$
$$A_s^{(-)}(0) = \frac{1}{2}\,(1-\widetilde{\alpha})\,A_s(0) - \frac{\widetilde{\beta}}{2}\,A_c(0) \tag{3.58}$$

$$A_c^{(+)}(0) = \frac{1}{2}\,(1-\widetilde{\alpha})\,A_c(0) + \frac{\widetilde{\gamma}}{2}\,A_s(0),$$
$$A_c^{(-)}(0) = \frac{1}{2}\,(1+\widetilde{\alpha})\,A_c(0) - \frac{\widetilde{\gamma}}{2}\,A_s(0) \tag{3.59}$$

and $A_{s,c}(0) = C_{s,c}(0)$.

In particular, if at $t = 0$ the synthetic axion is not excited, namely $A_s(0) = 0$, hybridization induces their excitations for $t > 0$, with amplitude in the Schrödinger picture

$$A_s(t) = \frac{1}{2}\,\widetilde{\beta}(E_s, E_c)\,(e^{-i\lambda^{+}t} - e^{-i\lambda^{-}t})\,C_c(0)\,, \tag{3.60}$$

similarly, if at $t = 0$ the cosmological axion is not excited but there is an excitation of the synthetic axion,

hybridization induces cosmological excitations for $t > 0$ with amplitude

$$A_c(t) = \tfrac{1}{2}\,\widetilde{\gamma}(E_s, E_c)\,(e^{-i\lambda^+ t} - e^{-i\lambda^- t})\,C_s(0)\,. \tag{3.61}$$

This is one of the main results of this study: excitations of synthetic axions are induced by the presence of cosmological axions or vice versa as a consequence of hybridization.

Inserting the above results in the equation for the coefficients $C_\kappa(t)$ of the intermediate states, Eq. (3.17) we find the amplitude for the two-photon state

$$C_\kappa(t) = [T_{\kappa s}\,A_s^{(+)}(0) + T_{\kappa c}\,A_c^{(+)}(0)]\left[\frac{1 - e^{i(E_\kappa - \varepsilon^+ + i\frac{\widetilde{\Gamma}^+}{2})t}}{E_\kappa - \varepsilon^+ + i\frac{\widetilde{\Gamma}^+}{2}}\right] + [T_{\kappa s}\,A_s^{(-)}(0) + T_{\kappa c}\,A_c^{(-)}(0)]\left[\frac{1 - e^{i(E_\kappa - \varepsilon^- + i\frac{\widetilde{\Gamma}^-}{2})t}}{E_\kappa - \varepsilon^- + i\frac{\widetilde{\Gamma}^-}{2}}\right]. \tag{3.62}$$

The probabilities for synthetic and cosmological axions feature interference terms,

$$|C_s(t)|^2 = |A_s^+(0)|^2\,e^{-\widetilde{\Gamma}^+ t} + |A_s^-(0)|^2\,e^{-\widetilde{\Gamma}^- t} + 2\mathrm{Re} \times \left[A_s^+(0)(A_s^-(0))^*\,e^{-i(\varepsilon^+ - \varepsilon^-)t}\,e^{-\frac{1}{2}(\widetilde{\Gamma}^+ + \widetilde{\Gamma}^-)t}\right], \tag{3.63}$$

with a similar expression for $|C_c(t)|^2$ with $A_s^\pm(0) \to A_c^\pm(0)$. The oscillatory interference terms are a consequence of hybridization, as can be seen explicitly since $A_s^-(0), A_c^+(0)$ vanish as $\widetilde{\beta}, \widetilde{\gamma} \to 0$, and are a manifestation of quantum beats. As a consequence of the unitarity relation (3.15) these quantum beats are also manifest in the probabilities $|C_\kappa(t)|^2$ of the intermediate states, and will be explicitly shown below. These results are general (in the Markov approximation) and complement and extend those of Refs. [35,36] by including the full contribution from the self-energy corrections, not just the imaginary parts.

Important checks. The validity of the description of hybridization can be confirmed with the following checks.

(i) Setting $C_c(0) = 0; g_c = 0$ the set of equations (3.6)–(3.8) simplifies to those obtained from the Weisskopf-Wigner description of spontaneous emission in a two levels atom [33], [similarly if $C_s(0) = 0; g_s = 0$].

(ii) Neglecting the real part of the self-energies, namely setting the Lamb shifts $\Delta_{ab} = 0$, recover the results of Refs. [35,36]. In particular, the mode described by the C_κ is equivalent to the pseudomode in Ref. [35].

The equivalence to the case of spontaneous emission in a two-level atom, obtained by setting $g_c = 0; C_c(0) = 0$ will prove important because the results obtained in the general case of hybridization will also apply to the case of just the synthetic emergent axion decaying into two photons. This result, a byproduct of the more general treatment with hybridization will be used in Sec. V to argue that two-photon HBT correlations may also be an important experimental probe of axion collective excitations in topological insulators and/or Weyl semimetals.

IV. SYNTHETIC AND COSMOLOGICAL AXION HYBRIDIZATION

In this section we apply the general results of the previous section to the hybridization of the synthetic and cosmological axions for which the interaction Hamiltonian to leading order in the couplings is given by Eq. (A31).

In interaction picture (see Appendix A) $\vec{E}(\vec{x}, t) = -\dot{\vec{A}}(\vec{x}, t)$, $\vec{B}(\vec{x}, t) = \vec{\nabla} \times \vec{A}(\vec{x}, t)$ and $\vec{A}(\vec{x}, t)$ is quantized in Coulomb gauge with the expansion (A26) with real (linear) polarization vectors. The pseduscalar fields $\phi_{s,c}(\vec{x}, t)$ in interaction picture are expanded as in Eq. (2.9).

We need the transition matrix elements

$$T_{s\kappa} = \langle 1_{\vec{k},s}|H_I(0)|\kappa\rangle \;;\; T_{c\kappa} = \langle 1_{\vec{k},c}|H_I(0)|\kappa\rangle\,, \tag{4.1}$$

where $|1_{\vec{k},s,c}\rangle$ are single-particle states of spatial momentum $\vec{k}$ of the synthetic and cosmological axions and the vacuum for the electromagnetic fields. Evidently the states $|\kappa\rangle$ are two-photon states of the form $|\kappa\rangle = |1_{\vec{k}_1,\lambda_1}, 1_{\vec{k}_2,\lambda_2}\rangle$ with $\vec{k}_2 = \vec{k} - \vec{k}_1$, and energy

$$E_\kappa \equiv E_{2\gamma} = k_1 + k_2\,. \tag{4.2}$$

Carrying out the spatial integral, we find the matrix elements for $a = s, c$

$$T_{a\kappa} \equiv \langle 1_{\vec{k},a}|H_I(0)|1_{\vec{k}_1,\lambda_1}, 1_{\vec{k}_2,\lambda_2}\rangle = \frac{g_a\,k_1 k_2}{2\sqrt{2\,E_a(k)V}}\,[\vec{\epsilon}_{\lambda_1}(\vec{k}_1)\cdot(\hat{\vec{k}}_2 \times \vec{\epsilon}_{\lambda_2}(\vec{k}_2)) + \vec{\epsilon}_{\lambda_2}(\vec{k}_2) \cdot (\hat{\vec{k}}_1 \times \vec{\epsilon}_{\lambda_1}(\vec{k}_1))]_{\vec{k}_2 = \vec{k} - \vec{k}_1}\,. \tag{4.3}$$

With sums replaced by integrals as

$$\sum_\kappa = \sum_{\vec{k}_1,\vec{k}_2}\sum_{\lambda_1,\lambda_2}, \quad \frac{1}{V}\sum_{\vec{k}_1} \to \int \frac{d^3k_1}{(2\pi)^3}\,, \tag{4.4}$$

the spectral density (3.29) becomes

$$\rho_{ab}(k_0; k) = \frac{g_a g_b}{4\sqrt{E_a(k)E_b(k)}}\int \frac{d^3k_1}{(2\pi)^3}\frac{1}{k_1|\vec{k} - \vec{k}_1|} \times [k_1|\vec{k} - \vec{k}_1| - \vec{k}_1\cdot(\vec{k} - \vec{k}_1)]^2 \times \delta(k_0 - k_1 - |\vec{k} - \vec{k}_1|)\,, \tag{4.5}$$

The details of its calculation are provided in Appendix B, with the result

$$\rho_{ab}(k_0; k) = \frac{g_a g_b}{32\pi^2\sqrt{E_a(k)E_b(k)}}\left(k_0^2 - k^2\right)^2\Theta(k_0 - k)\,, \tag{4.6}$$

yielding for the real and imaginary parts of the self-energy matrix

$$\Delta_{ss}(E_s) = \frac{g_s^2}{32\pi^2 E_s(k)}\int_k^\Lambda \mathcal{P}\Big[\frac{\left(k_0^2 - k^2\right)^2}{E_s - k_0}\Big],$$

$$\Gamma_{ss}(E_s) = \frac{g_s^2\left(E_s^2(k) - k^2\right)^2}{16\pi E_s(k)}\,,$$

$$\Delta_{cc}(E_c) = \frac{g_c^2}{32\pi^2 E_c(k)}\int_k^\Lambda \mathcal{P}\Big[\frac{\left(k_0^2 - k^2\right)^2}{E_c - k_0}\Big],$$

$$\Gamma_{cc}(E_c) = \frac{g_c^2\, m_c^2}{16\pi E_c(k)}\,,$$
$$\Delta_{sc}(E_c) = \frac{g_s g_c}{32\pi^2\sqrt{E_s(k)E_c(k)}}\int_k^\Lambda \mathcal{P}\Big[\frac{\left(k_0^2-k^2\right)^2}{E_c-k_0}\Big],$$
$$\Gamma_{sc}(E_c) = \frac{g_s g_c\, m_c^2}{16\pi\sqrt{E_s(k)E_c(k)}}\,,$$
$$\Delta_{cs}(E_s) = \frac{g_s g_c}{32\pi^2\sqrt{E_s(k)E_c(k)}}\int_k^\Lambda \mathcal{P}\Big[\frac{\left(k_0^2-k^2\right)^2}{E_s-k_0}\Big],$$
$$\Gamma_{cs}(E_s) = \frac{g_s g_c\left(E_s^2(k)-k^2\right)^2}{16\pi\sqrt{E_s(k)E_c(k)}}\,, \tag{4.7}$$

where we have introduced an upper cutoff Λ in the integrals for the real parts (Lamb shifts Δ_{ab}) to highlight that all these contributions are ultraviolet divergent in the $\Lambda\to\infty$ limit requiring renormalization, an aspect that will be discussed in Sec. VI.

We are particularly interested in the amplitude of the two-photon state (3.62), which becomes

$$C_{2\gamma}(\vec{k}_1,\lambda_1;\vec{k}_2,\lambda_2;t) = \Bigg\{\mathcal{A}^+\Bigg[\frac{1-e^{i(E_{2\gamma}-\varepsilon^+ +i\frac{\widetilde{\Gamma}^+}{2})t}}{E_{2\gamma}-\varepsilon^+ +i\frac{\widetilde{\Gamma}^+}{2}}\Bigg] + \mathcal{A}^-\Bigg[\frac{1-e^{i(E_{2\gamma}-\varepsilon^- +i\frac{\widetilde{\Gamma}^-}{2})t}}{E_{2\gamma}-\varepsilon^- +i\frac{\widetilde{\Gamma}^-}{2}}\Bigg]\Bigg\} \times \mathcal{C}(\vec{k}_1,\lambda_1;\vec{k}_2,\lambda_2)\,, \tag{4.8}$$

where $E_{2\gamma} = k_1 + |\vec{k}-\vec{k}_1|$, and the amplitudes $\mathcal{A}^\pm$ are given by

$$\mathcal{A}^+ = \frac{k_1|\vec{k}-\vec{k}_1|}{\sqrt{8V}}\Bigg[\frac{g_s A_s^{(+)}(0)}{\sqrt{E_s(k)}}+\frac{g_c A_c^{(+)}(0)}{\sqrt{E_c(k)}}\Bigg] \tag{4.9}$$
$$\mathcal{A}^- = \frac{k_1|\vec{k}-\vec{k}_1|}{\sqrt{8V}}\Bigg[\frac{g_s A_s^{(-)}(0)}{\sqrt{E_s(k)}}+\frac{g_c A_c^{(-)}(0)}{\sqrt{E_c(k)}}\Bigg], \tag{4.10}$$

with $A^\pm_{s,c}(0)$ given by Eqs. (3.58), (3.59). The function

$$\mathcal{C}(\vec{k}_1,\lambda_1;\vec{k}_2,\lambda_2) = \big[\vec{\epsilon}_{\lambda_1}(\vec{k}_1)\cdot\big(\hat{\vec{k}}_2\times\vec{\epsilon}_{\lambda_2}(\vec{k}_2)\big)+\vec{\epsilon}_{\lambda_2}(\vec{k}_2) \cdot\big(\hat{\vec{k}}_1\times\vec{\epsilon}_{\lambda_1}(\vec{k}_1)\big)\big],\quad \vec{k}_2=\vec{k}-\vec{k}_1\,, \tag{4.11}$$

contains all the polarization information of the photon pair, depends only on the direction of the wave vectors, and is symmetric under the exchange $\vec{k}_1,\lambda_1 \Leftrightarrow \vec{k}_2,\lambda_2$, which implies that

$$C_{2\gamma}(\vec{k}_1,\lambda_1;\vec{k}_2,\lambda_2;t) = C_{2\gamma}(\vec{k}_2;\lambda_2,\vec{k}_1,\lambda_1;t)\,. \tag{4.12}$$

The two-photon state

$$|\psi_{2\gamma}(t)\rangle = \sum_{\vec{k}_1,\lambda_1,\lambda_2} C_{2\gamma}(\vec{k}_1,\lambda_1;\vec{k}_2,\lambda_2;t)\,\Big|1^\gamma_{\vec{k}_1,\lambda_1};1^\gamma_{\vec{k}_2,\lambda_2}\Big\rangle;\quad \vec{k}_2=\vec{k}-\vec{k}_1\,, \tag{4.13}$$

is entangled both in momentum and polarization with two noteworthy aspects:

(i) The resonant denominators in the amplitudes (4.8), entail that the probability $|C_{2\gamma}(\vec{k}_1,\lambda_1,\vec{k}_2,\lambda_2;t)|^2$ of finding a photon pair with momenta $\vec{k}_1,\vec{k}_2=\vec{k}-\vec{k}_1$ features two peaks, at the values $k_1+|\vec{k}-\vec{k}_1|\simeq\varepsilon^\pm$, which are the kinematic regions of energy conserving transitions. If $|\varepsilon^+-\varepsilon^-|\lesssim\Gamma^++\Gamma^-$ the two peaks blur into one, this is the (unlikely) case when the synthetic and cosmological axions are nearly degenerate (see discussion below).

(ii) To highlight polarization entanglement in a clear manner, let us consider the case $\vec{k}=0$, namely $\vec{k}_2=-\vec{k}_1$ corresponding to back-to-back photons. In this case the coefficient (4.11) becomes

$$\mathcal{C}(\vec{k}_1,\lambda_1;-\vec{k}_1,\lambda_2) = [\vec{\epsilon}_{\lambda_1}(\vec{k}_1)\cdot(-\hat{\vec{k}}_1\times\vec{\epsilon}_{\lambda_2}(-\vec{k}_1)) + \vec{\epsilon}_{\lambda_2}(-\vec{k}_1)\cdot(\hat{\vec{k}}_1\times\vec{\epsilon}_{\lambda_1}(\vec{k}_1))]\,, \tag{4.14}$$

using the properties (A27) of the polarization vectors, we find that if $\lambda_1=1$ then $\lambda_2=2$ for the amplitude to be nonvanishing, and viceversa, implying that the photons are emitted back to back and with perpendicular polarizations. In other words, the emitted photons feature telltale correlations both in momenta and in polarization. The polarization dependence of the coefficient $\mathcal{C}(\vec{k}_1,\lambda_1;\vec{k}_2,\lambda_2)$ in Eq. (4.11) is a distinct manifestation of the pseudoscalar coupling to electromagnetism via the Chern-Simons term.

HBT correlations (second-order coherence):

The characteristics of the two-photon state may be probed with intensity interferometry as per Glauber's theory of photodetection [39] with the Hanbury Brown-Twiss [40] (HBT) second-order coherence for coincident photodetection

$$G^{(2)}(\vec{x}_1,t;\vec{x}_2,t) = \langle\psi(t)|E^-(\vec{x}_2,t)E^-(\vec{x}_1,t)E^+ \times(\vec{x}_1,t)E^+(\vec{x}_2,t)|\psi(t)\rangle\,, \tag{4.15}$$

(we suppressed the vector labels) where

$$\vec{E}^-(\vec{x},t) = \frac{-i}{\sqrt{V}}\sum_{\vec{k},\lambda=1,2}\sqrt{\frac{k}{2}}\,\vec{\epsilon}_\lambda(\vec{k})\,a^\dagger_{\vec{k},\lambda}\,e^{i(\vec{k}\cdot\vec{x}-kt)}\,, \tag{4.16}$$
$$\vec{E}^+(\vec{x},t) = \frac{i}{\sqrt{V}}\sum_{\vec{k},\lambda=1,2}\sqrt{\frac{k}{2}}\,\vec{\epsilon}_\lambda(\vec{k})\,a_{\vec{k},\lambda}\,e^{-i(\vec{k}\cdot\vec{x}-kt)}\,. \tag{4.17}$$

As discussed above, the two-photon state features correlations both in momentum and polarization. However, the operators (4.16), (4.17) are sums of both observables, hence, the spatiotemporal second-order coherence (4.15) probes momentum and polarization entanglement only indirectly. Following Ref. [41] we introduce instead the momentum- and polarization-resolved operators

$$\mathcal{O}^-_{\vec{p},s}(t) = \sqrt{\frac{1}{V}}\int\vec{\epsilon}_s(\vec{p})\cdot\vec{E}^-(\vec{x},t)\,e^{-i\vec{p}\cdot\vec{x}}\,d^3x\,, \tag{4.18}$$
$$\mathcal{O}^+_{\vec{p},s}(t) = \sqrt{\frac{1}{V}}\int\vec{\epsilon}_s(\vec{p})\cdot\vec{E}^+(\vec{x},t)\,e^{i\vec{p}\cdot\vec{x}}\,d^3x\,, \tag{4.19}$$

which are directly related to the photon annihilation and creation operators as

$$\mathcal{O}^-_{\vec{p},s}(t) = \sqrt{\frac{p}{2}}\,a_{\vec{p},s}\,e^{-ikt},\quad \mathcal{O}^+_{\vec{p},s}(t) = \sqrt{\frac{p}{2}}\,a^\dagger_{\vec{p},s}\,e^{ikt}\,. \tag{4.20}$$

Instead of the spatiotemporal (HBT) correlation (4.15), and following Ref. [41] we obtain the momentum- and polarization-resolved cross correlation (second-order cross-spectral density)[3]

$$\widetilde{G}^{(2)}(\vec{p}_1, s_1; \vec{p}_2, s_2; t) = \langle \psi(t)| a^{\dagger}_{\vec{p}_1,s_1} a^{\dagger}_{\vec{p}_2,s_2} a_{\vec{p}_2,s_2} a_{\vec{p}_1,s_1} |\psi(t)\rangle \,, \tag{4.21}$$

from which the full spatiotemporal second-order coherence (4.15) may be obtained. Using the symmetry (4.12) we find

$$\widetilde{G}^{(2)}(\vec{p}_1, s_1; \vec{p}_2, s_2; t) = 4\,|C_{2\gamma}(\vec{p}_1, s_1; \vec{p}_2, s_2; t)|^2\, \delta_{\vec{p}_1+\vec{p}_2,\vec{k}} \,. \tag{4.22}$$

It is straightforward to obtain also the first-order cross correlation

$$\widetilde{G}^{(1)}(\vec{p}_1, s_1; \vec{p}_2, s_2; t) = \langle \psi(t)| a^{\dagger}_{\vec{p}_1,s_1} a_{\vec{p}_2,s_2} |\psi(t)\rangle \,, \tag{4.23}$$

however, the result is neither very illuminating nor useful as a probe of polarization because it entails the sum over one of the polarizations and averages over the polarization information. However, for completeness this correlation function is obtained in Appendix C.

Therefore, we propose the momentum- and polarization-resolved two-photon (HBT) cross correlation (4.21) as a possible experimental probe of both momentum and polarization entanglement with the distinct polarization correlations determined by the pseudoscalar coupling, a telltale sign of axion electrodynamics encoded in the coefficient (4.11).

Armed with the general result (4.8) we find

$$\begin{aligned}\widetilde{G}^{(2)}(\vec{p}_1, s_1; \vec{p}_2, s_2; t) = 4\,\{&|\mathcal{A}^+|^2\, D^+(\vec{p}_1; t) + |\mathcal{A}^-|^2\, D^-(\vec{p}_1; t) \\ &+ (\mathcal{A}^+)^* \mathcal{A}^-\, I[\vec{p}_1; t] + \text{c.c.}\} \\ &\times \mathcal{C}^2(\vec{p}_1, s_1; \vec{p}_2, s_2)\end{aligned} \tag{4.24}$$

were $\vec{p}_2 = \vec{k} - \vec{p}_1$. The direct term D^+ is given by

$$D^+(\vec{p}_1; t) = \frac{\left[1 - (e^{i(E_{2\gamma}-\varepsilon^+)t} + e^{-i(E_{2\gamma}-\varepsilon^+)t})\, e^{-\frac{\widetilde{\Gamma}^+}{2}t} + e^{-\widetilde{\Gamma}^+ t}\right]}{(E_{2\gamma} - \varepsilon^+)^2 + \left(\frac{\widetilde{\Gamma}^+}{2}\right)^2} \,, \tag{4.25}$$

with a similar expression for $D^-(\vec{p}_1; t)$ with the substitution $\varepsilon^+ \,,\ \widetilde{\Gamma}^+ \to \varepsilon^- \,,\ \widetilde{\Gamma}^-$. The interference term is given by

$$I[\vec{p}_1; t] = \frac{1 - e^{-i(E_{2\gamma}-\varepsilon^+)t}\, e^{-\frac{\widetilde{\Gamma}^+}{2}t} - e^{i(E_{2\gamma}-\varepsilon^-)t}\, e^{-\frac{\widetilde{\Gamma}^-}{2}t} + e^{i(\varepsilon^+-\varepsilon^-)t}\, e^{-\frac{(\widetilde{\Gamma}^+ + \widetilde{\Gamma}^-)}{2}t}}{(E_{2\gamma} - \varepsilon^+ - i\frac{\widetilde{\Gamma}^+}{2})(E_{2\gamma} - \varepsilon^- + i\frac{\widetilde{\Gamma}^-}{2})} \,. \tag{4.26}$$

The direct and interference terms are dominated by the region of $E_{2\gamma}$ near the resonances, namely $E_{2\gamma} \simeq \varepsilon^{\pm}$, and the interference term displays the quantum beats with typical frequency $\varepsilon^+ - \varepsilon^-$. The dominant part of the direct and interference terms can be made more explicit by filtering the cross correlation in frequency near the resonances.

Momentum or frequency-resolved (filtered) HBT correlations including cross-correlations of the form (4.21) have been experimentally studied as a colored HBT in Ref. [42] where the source of light is a polariton condensate. This experiment demonstrates the feasibility of frequency resolution in intensity interferometry, suggesting the possible experimental feasibility of the momentum- and polarization-resolved HBT cross correlation (4.22) to probe two-photon correlated states from the hybridization of synthetic and cosmological axions.

The contributions to the HBT cross correlation $\widetilde{G}^{(2)}$ while not being monochromatic, are dominated by the respective resonant denominators, however, photodetectors feature a finite resolution, therefore following the filtering procedure of Ref. [42] we integrate this correlation in frequency (or $E_{2\gamma}$), but not in direction so as to maintain the polarization dependence, within a small band of width ξ (determined by the photodetector resolution) around the resonances $\xi < |E_{2\gamma} - \varepsilon|$ with $\Gamma^{\pm} \ll \xi \ll E_{2\gamma}$. Assuming very narrow widths $\Gamma^{\pm}$ for weak couplings, we extend the integration region to infinity and carry out the integration by contour integration in the complex frequency plane[4] as in Refs. [33,43].

For terms containing exponentials of the form $e^{i(E_{2\gamma}-\varepsilon^+)t}$ ($e^{-i(E_{2\gamma}-\varepsilon^+)t}$) the contour is closed in the upper (lower) half frequency plane yielding for the integration of the direct and interference terms in $\widetilde{G}^{(2)}$

$$D^+(\vec{p}_1; t) \simeq 2\pi\, \frac{1 - e^{-\Gamma^+ t}}{\Gamma^+} \,, \quad D^-(\vec{p}_1; t) \simeq 2\pi\, \frac{1 - e^{-\Gamma^- t}}{\Gamma^-} \,, \tag{4.27}$$

$$I[\vec{p}_1; t] \simeq 2\pi\, i \left[\frac{1 - e^{i(\varepsilon^+ - \varepsilon^-)t}\, e^{-(\widetilde{\Gamma}^+ + \widetilde{\Gamma}^-)\frac{t}{2}}}{\varepsilon^+ - \varepsilon^- + \frac{i}{2}(\widetilde{\Gamma}^+ + \widetilde{\Gamma}^-)}\right] . \tag{4.28}$$

Gathering all the terms, upon filtering in a narrow band of frequencies near the resonances we find the final form of the second-order cross correlation

$$\begin{aligned}\widetilde{G}^{(2)}(\vec{p}_1, s_1; \vec{p}_2, s_2; t) \propto \Bigg\{ &\frac{|\mathcal{A}^+|^2}{\Gamma^+}(1 - e^{-\Gamma^+ t}) + \frac{|\mathcal{A}^-|^2}{\Gamma^-} \\ &\times (1 - e^{-\Gamma^- t}) + i\,(\mathcal{A}^+)^* \mathcal{A}^- \\ &\times \left[\frac{1 - e^{i(\varepsilon^+ - \varepsilon^-)t}\, e^{-(\widetilde{\Gamma}^+ + \widetilde{\Gamma}^-)\frac{t}{2}}}{\varepsilon^+ - \varepsilon^- + \frac{i}{2}(\widetilde{\Gamma}^+ + \widetilde{\Gamma}^-)}\right] \\ &+ \text{c.c}\Bigg\} \mathcal{C}^2(\vec{p}_1, s_1; \vec{p}_2, s_2).\end{aligned} \tag{4.29}$$

The polarization function $\mathcal{C}(\vec{p}_1, s_1; \vec{p}_2, s_2)$ only depends on the directions of the vectors, which have not been integrated over so that polarization information is maintained after frequency integration within the photodetector band width. The last term inside the brackets in the final result (4.29), arising from the interference contribution $I[\vec{p}_1; t]$ displays the quantum

[3] See Chap. 12.5.2 in Ref. [41].

[4] See a similar treatment in Chap. 6.3 of Ref. [33].

beats. A noteworthy aspect of the above results is that, the ratios $|\mathcal{A}^{\pm}|^2/\Gamma^{\pm}$ are of $\mathcal{O}(1)$ in the couplings, whereas the interference term is quadratic in the couplings, however, it is enhanced in the (unlikely) nearly degenerate case when $|\varepsilon^+ - \varepsilon^-|$ is of order $g_s^2, g_c^2, g_s g_c$.

Nondegenerate limit. The results (4.8) and (4.29) are general and valid for arbitrary small couplings g_s, g_c and masses m_s, m_c. However, it is very unlikely that the masses of the synthetic and cosmological axions be nearly degenerate and of the same order as the self-energy corrections $\Sigma_{ab}, a, b = s, c$ in the expressions (3.35), (3.36). Neglecting the possibility of a (very unlikely) coincidence of the masses, we consider that $|E_s - E_c| \gg \Sigma_{ab}$ since the self-energy matrix is of quadratic order in the small couplings, referring to this case as the nondegenerate limit. With this assumption the expressions for (3.36)–(3.39) simplify to

$$\widetilde{D}(E_s, E_c) \simeq |E_s + \Sigma_{ss}(E_s) - E_c - \Sigma_{cc}(E_c)| + \mathcal{O}\big(g_s^2 g_c^2\big) \tag{4.30}$$

$$\widetilde{\alpha}(E_s, E_c) \simeq 1 + \mathcal{O}\big(g_s^2 g_c^2\big),$$
$$\widetilde{\beta}(E_s, E_c) \simeq \mathcal{O}(g_s g_c)\widetilde{\gamma}(E_s, E_c) \simeq \mathcal{O}(g_s g_c)\,. \tag{4.31}$$

In the following analysis we will consider that $E_s > E_c$, corresponding to the choice $\widetilde{\alpha}(E_s, E_c) \simeq 1$, in this non-degenerate limit, the case $E_c > E_s$ can be obtained from straightforward replacements.

In this limit the (quasi)normal mode eigenvalues are given by

$$\lambda^+ = E_s + \Sigma_{ss}(E_s) + \mathcal{O}\big(g_s^2 g_c^2\big)\,, \tag{4.32}$$

$$\lambda^- = E_c + \Sigma_{cc}(E_c) + \mathcal{O}\big(g_s^2 g_c^2\big)\,, \tag{4.33}$$

where the real and imaginary parts of the self-energies are given by Eq. (3.32). The real part of the diagonal matrix elements of the self-energy correspond to renormalizations of $E_{s,c}$ (Lamb shifts), and are absorbed into the renormalized energies

$$E_s^r = E_s + \Delta_{ss}(E_s); E_c^r = E_c + \Delta_{cc}(E_c)\,, \tag{4.34}$$

therefore, in the nondegenerate limit we find the (quasi)normal mode frequencies

$$\lambda^+ = E_s^r - i\frac{\Gamma_{ss}}{2}, \quad \Gamma_{ss} = 2\pi\rho_{ss}(E_s)\,, \tag{4.35}$$

$$\lambda^- = E_c^r - i\frac{\Gamma_{cc}}{2}, \quad \Gamma_{cc} = 2\pi\rho_{cc}(E_c)\,, \tag{4.36}$$

where the diagonal matrix elements of the spectral density ρ_{ab} and decay widths can be read off Eqs. (4.7).

Since the matrix elements $T_{a\kappa}$ given by Eq. (4.3) are of order g_a, it follows that we can replace the amplitudes (3.58), (3.59) in Eq. (3.62) by their leading order in the couplings, namely

$$A_s^{(+)}(0) \simeq A_s(0) = C_s(0), \quad A_s^{(-)}(0) \simeq 0 \tag{4.37}$$

$$A_c^{(+)}(0) \simeq 0, \quad A_c^{(-)}(0) \simeq A_c(0) = C_c(0)\,. \tag{4.38}$$

In this approximation the two-photon amplitude (4.8) becomes

$$C_{2\gamma}(\vec{p}_1, s_1; \vec{p}_2, s_2; t) = \left\{ \frac{g_s\, C_s(0)}{\sqrt{E_s(k)}} \left[\frac{1 - e^{i(E_{2\gamma} - E_s^r + i\frac{\Gamma_{ss}}{2})t}}{E_{2\gamma} - E_s^r + i\frac{\Gamma_{ss}}{2}} \right] + \frac{g_c\, C_c(0)}{\sqrt{E_c(k)}} \left[\frac{1 - e^{i(E_{2\gamma} - E_c^r + i\frac{\Gamma_{cc}}{2})t}}{E_{2\gamma} - E_c^r + i\frac{\Gamma_{cc}}{2}} \right] \right\} \times \mathcal{C}(\vec{p}_1, s_1; \vec{p}_2, s_2)\, \delta_{\vec{p}_2, \vec{k} - \vec{p}_1}\,,$$
$$E_{2\gamma} = p_1 + p_2\,. \tag{4.39}$$

We note that in keeping only the leading terms in the couplings, we have neglected the induced amplitudes (3.60), (3.61) which are a consequence of hybridization and suppressed by the product $g_s g_c$ with respect to the leading order terms in the nondegenerate limit. However, if either of the initial amplitudes $C_{s,c}(0)$ vanish, these subleading induced terms must be kept, since these will be the source of interference and quantum beats.

In this nondegenerate case, and assuming initial amplitudes $C_s(0) \neq 0; C_c(0) \neq 0$, the frequency-filtered second-order cross correlation (4.29) becomes

$$\widetilde{G}^{(2)}(\vec{p}_1, s_1; \vec{p}_2, s_2; t) \propto \left\{ \frac{g_s^2\, |C_s(0)|^2}{E_s(k)\Gamma_{ss}}(1 - e^{-\Gamma_{ss}t}) + \frac{g_c^2\, |C_c(0)|^2}{E_c(k)\Gamma_{cc}}(1 - e^{-\Gamma_{cc}t}) + i\,\frac{g_s g_c C_s^*(0) C_c(0)}{\sqrt{E_s(k)E_c(k)}} \left[\frac{1 - e^{i(E_s^r - E_c^r)t}\, e^{-(\Gamma_{ss} + \Gamma_{cc})\frac{t}{2}}}{E_s^r - E_c^r + \frac{i}{2}(\Gamma_{ss} + \Gamma_{cc})} \right] + \text{c.c.} \right\} \mathcal{C}^2(\vec{p}_1, s_1; \vec{p}_2, s_2)\,, \tag{4.40}$$

with $\mathcal{C}(\vec{p}_1, s_1; \vec{p}_2, s_2)$ being the polarization function (4.11). The quantum beats are explicit in the third, interference term with the beat frequency being the difference between the (renormalized) synthetic and cosmological axion energies. This is one of the main results of our study.

V. DETECTING SYNTHETIC AXIONS WITH HBT

The discussion above focused on understanding the consequences of hybridization between synthetic and cosmological axions, such as momentum and polarization entanglement and in particular quantum beats as a manifestation of interference. However, momentum and polarization entanglement are characteristics of the process of axion decay that apply individually to each species independently of their hybridization. Kinematic entanglement is a consequence of energy-momentum conservation, and the particular pattern of polarization entanglement is solely a consequence of the Chern-Simons coupling to electromagnetism, which is common to both species of axions. This is explicit in the

expression (4.40) where the polarization-dependent function $\mathcal{C}$ multiplies all the terms.

The feebleness of the coupling of cosmological axions to electromagnetism [9,10,13,14] may result in a quantum beat signal, the third term in Eq. (4.40) (valid in the nondegenerate case), to be too small to be detected. However, even in this case, the analysis above unambiguously suggests that momentum and polarization-resolved HBT second-order coherence may be a useful experimental probe to detect synthetic axions independently.

The case of synthetic axions only can be obtained from the nondegenerate limit straightforwardly by setting $g_c = 0$, yielding $\widetilde{\alpha}(E_s, E_c) = 1, \widetilde{\beta} = 0, \widetilde{\gamma} = 0$ and $\varepsilon^+ = E_s^r$. Therefore, the two-photon amplitude (4.39) from synthetic axion decay becomes

$$C_{2\gamma}(\vec{p}_1, s_1; \vec{p}_2, s_2; t) = \frac{g_s\, C_s(0)}{\sqrt{E_s(k)}}\left[\frac{1 - e^{i(E_{2\gamma} - E_s^r + i\frac{\Gamma_{ss}}{2})t}}{E_{2\gamma} - E_s^r + i\frac{\Gamma_{ss}}{2}}\right] \times \mathcal{C}(\vec{p}_1, s_1; \vec{p}_2, s_2)\, \delta_{\vec{p}_2, \vec{k} - \vec{p}_1}\,,$$
$$E_{2\gamma} = p_1 + p_2\,, \tag{5.1}$$

and the frequency-filtered second-order cross correlation (4.40) becomes

$$\widetilde{G}^{(2)}(\vec{p}_1, s_1; \vec{p}_2, s_2; t) \propto \frac{2\pi\, g_s^2\, |C_s(0)|^2}{E_s \Gamma_{ss}}(1 - e^{-\Gamma_{ss} t}) \times \mathcal{C}^2(\vec{p}_1, s_1; \vec{p}_2, s_2)\,. \tag{5.2}$$

The distinct pattern of polarization entanglement, determined by the function $\mathcal{C}$ in (5.2) and momentum entanglement are features of the two-photon state from synthetic axion decay independently of the hybridization with the cosmological axion. Therefore our argument above suggests that coincident two-photon photodetection with momentum and polarization resolution via the HBT second-order coherence or cross correlation is a robust tool to seek signatures of synthetic axions. HBT second-order coherence may provide a useful diagnostic tool complementing the proposal in Ref. [44] for multiphoton detection as a probe of axionic collective excitations in topological insulators or Weyl semimetals.

Similarities and differences with parametric down conversion

The results in the previous sections bear a striking similarity to the phenomenon of parametric down conversion [45–47]. In this process an incoming beam of photons from a laser (pump) propagate in a nonlinear medium and split into two lower-frequency signal and idler photons through a nonlinear second-order susceptibility tensor χ_{ijk}. The interaction Hamiltonian is modeled with a cubic-type electromagnetic vertex $\propto \chi_{ijk} E_i^P E_j^S E_k^I$, with P, S, I for pump, signal, and idler fields [45–47]. For an intense monochromatic laser beam, the pump field is usually taken to be classical whereas the signal and idler fields are quantized. The two photons emerging from the nonlinear crystal (signal and idler) feature momentum and polarization entanglement as a consequence of the nonlinearity similarly to the two photons emerging from axion decay. The down conversion is of type I or type II, respectively, if the photon pair features parallel or perpendicular polarizations.

In a finite-sized crystal and during a finite time interval, the momenta and frequencies of the signal and idler photons are determined by the sinc-type functions [45]

$$\Pi_{m=1}^3\left[\frac{\sin\left[\frac{1}{2}(\vec{k}_P - \vec{k}_S - \vec{k}_I)_m L_m\right]}{\frac{1}{2}(\vec{k}_P - \vec{k}_S - \vec{k}_I)_m}\right] \times \frac{\sin\left[\frac{1}{2}(\omega_P - \omega_S - \omega_I)t\right]}{\frac{1}{2}(\omega_P - \omega_S - \omega_I)}\,, \tag{5.3}$$

which for large size in each direction L_m and for large time t yield the (approximate) phase and frequency matching conditions

$$\vec{k}_P \simeq \vec{k}_S + \vec{k}_I\,, \quad \omega_P \simeq \omega_S + \omega_I\,. \tag{5.4}$$

These conditions must be compared to the momentum conservation condition in axion decay $\vec{k}_1 + \vec{k}_2 = \vec{k}$ in the results of the previous section and the resonant denominators in the amplitude (4.8), which yield the largest amplitude for the energy-conserving conditions $E_{2\gamma} \simeq \varepsilon^{\pm}$. In the limit of vanishing width these resonant denominators can be replaced by approximate energy-conserving delta functions, the blurring of the energy-conserving condition is a consequence of the uncertainty associated with the lifetime of the decaying state. The time-dependent sinc function in (5.3) is the usual function arising in time-dependent perturbation theory that yields energy conservation in the long-time limit in the mode of Fermi's golden rule. Therefore the kinematic constraints from parametric down conversion (phase and frequency matching) are equivalent to those in the two-photon final state from axion decay, this is of course expected from the kinematics of energy-momentum conservation. The main difference is in the polarization entanglement. Whereas for axion decay, the polarization function consequence of polarization entanglement is given by Eq. (4.11), in parametric down conversion the dependence in the polarization is given by a function of the form [45]

$$\mathcal{C}(\vec{k}_S, \lambda_S; \vec{k}_I, \lambda_I) \propto \widetilde{\chi}_{ijl}\, \vec{\epsilon}_j(\vec{k}_S)\, \vec{\epsilon}_l(\vec{k}_I)\,, \tag{5.5}$$

where $\widetilde{\chi}$ is a frequency Fourier transform of the nonlinear susceptibility.

These differences notwithstanding, the main remarkable similarity between axion decay and parametric down conversion is that of momentum and polarization entanglement in the final two-photon state. In Refs. [45–47] second-order (intensity) interferometry, with HBT second-order coherences, has been proposed to study the correlations between signal and idler photons, in either type of parametric down conversion. And in Ref. [48] polarization-resolved HBT second-order coherence was used to test violations of Bell inequalities in a two-photon correlation experiment from the interference of signal and idler photons from parametric down conversion.

Therefore the main similarity between the case of condensed matter and cosmological axions and parametric down conversion bolsters the argument anticipated in the previous section that HBT second-order coherence, perhaps with momentum and polarization resolution, may be suitable probes for detection of both synthetic and cosmological axions. In the case of hybridization these intensity correlations will feature quantum beats. Furthermore, even in the case when the

cosmological coupling g_c is so small so as to make the quantum beats unobservable, both momentum and polarization correlations in the two-photon final state are a distinct telltale sign of axionic excitations in topological insulators and in Weyl semimetals, which are imprinted in the second-order HBT correlations. Therefore, axionic collective excitations in condensed matter systems may be probed with intensity interferometry via momentum- and polarization-resolved second-order HBT cross correlations.

VI. DISCUSSION

Beyond the Markov approximation. In our analysis, we have taken the Markovian limit in the form of the long-time limit in equation (3.28). This is ubiquitous and familiar in the Weisskopf-Wigner theory of spontaneous emission in single or multilevel atoms [33–37]. Keeping the full time dependence entails a time-dependent 2×2 Hamiltonian, and the solution of the effective Schrödinger equation involves the time-ordered exponential of this Hamiltonian, with obvious technical complications. The time dependence of the Hamiltonian may affect the early time, transient dynamics, but for weak coupling we expect the intermediate and long-time dynamics to be reliably described by the Markovian limit. Of course this expectation must be analyzed and confirmed with a rigorous calculation, which is beyond the main objectives of this article and is postponed to further study.

Renormalization of the real part of the self-energy (Lamb shift). The real part of the self-energy matrix Δ_{ab}, given by equation (3.32) is divergent in the limit of large ultraviolet cutoff scale Λ. The diagonal matrix elements Δ_{ss}, Δ_{cc} correspond to Lamb shifts and are absorbed into a renormalization of the single-particle energies for synthetic and cosmological axions, as in Eq. (4.34). However, the off-diagonal matrix elements cannot be absorbed by any terms in the (bare) Lagrangian as there are no bare terms in the Lagrangian density that mix the synthetic and cosmological excitations. In principle, to renormalize these terms the bare Lagrangian density must be extended to include local off-diagonal (mass-type) terms that mix synthetic and cosmological axions as counterterms of order $g_s g_c$, which are then chosen to cancel the divergences in the off-diagonal terms Δ_{sc}, Δ_{cs}. In the nondegenerate case studied in the previous sections (and the most likely scenario), the contributions from the off-diagonal self-energy matrix elements are subleading and their renormalization is not needed to leading order in the couplings as derived in the previous sections. However, in the (unlikely) case in which the energy differences are of the order of or smaller than the self-energy corrections, the full renormalization program including counterterms in the bare Lagrangian must be addressed. This theoretical possibility merits further and deeper study, again a technical aspect that is well beyond the realm of our objectives here.

Nearly degenerate case. There is a wide range of masses for the cosmological axion that are phenomenologically viable [9,10,13,14], $10^{-21}\,\text{eV} \lesssim m_c \lesssim \text{GeV}$ with the low end favored for ultralight dark matter, whereas the mass range for synthetic axions, typically determined by the material properties is within the meV [17,18]. Therefore, unless there is a coincidence, synthetic and cosmological axions are unlikely to be nearly degenerate, namely with a difference in masses of the same order as the self-energy corrections, which are perturbatively small for small coupling. The results (4.39), (4.40) were obtained under the assumption that synthetic and cosmological axions are not nearly degenerate so that the product of off-diagonal self-energy matrix elements in (3.36) and the off-diagonal coefficients in (3.37) can be safely neglected.

If both axions are nearly degenerate these contributions can no longer be neglected and the full dispersion relations of the (quasi)normal modes must be worked out in detail. While this by itself is an interesting but complicated theoretical exercise, we do not consider this possibility to be realistic and focused on the most likely nondegenerate scenario to highlight the main physical phenomena of hybridization and its consequences.

Induced synthetic axion condensate. A corollary of hybridization is that even if the initial amplitude of one of the axion species vanishes, it is generated upon time evolution, as described by equations (3.60), (3.61). In the nondegenerate case, the main focus of the discussion in the previous sections, the coefficients $\widetilde{\beta}; \widetilde{\gamma}$ in Eqs. (3.60), (3.61) are perturbatively small and of order $g_s g_c$, but are enhanced to be of $\mathcal{O}(1)$ in the nearly degenerate case. A current cosmological paradigm posits that dark matter is in the form of a spatially homogeneous but time-dependent cosmological axion condensate [9,10,13]. Hybridization entails that such condensate induces a condensate of axionic excitations in topological insulators or Weyl semimetals. Accordingly, this should translate into HBT correlations and coincident photodetection with a characteristic polarization pattern even if axionic collective excitations are not generated by the experimental setup. This is certainly an intriguing possibility for indirect detection of axionic dark matter, which excites the collective axionic modes in these condensed matter platforms via the hybridization mechanism.

VII. CONCLUSIONS AND FURTHER QUESTIONS

Cosmological axions (ϕ_c), a compelling dark matter candidate, and synthetic axions (ϕ_s), emergent collective excitations in topological insulators and in Weyl semimetals couple to electromagnetism via a (pseudoscalar) Chern-Simons term. Their mutual coupling to electromagnetism implies that both species of axions hybridize via the emission and absorption of two photons $\phi_c \Leftrightarrow 2\gamma \Leftrightarrow \phi_s$, resulting in an off-diagonal self-energy matrix.

An analogy with a three-level V-type atomic system, identifying the two upper levels with the synthetic and cosmological axions decaying to a ground level via two-photon emission leads us to generalize and extend the Weisskopf-Wigner theory of spontaneous emission in multilevel atoms to study the dynamics of hybridization and its consequences. This formulation allows us to obtain the final two-photon state, which features momentum and polarization entanglement and quantum beats as a consequence of the interference between the decay paths.

A two-photon correlated final state motivates us to obtain a second-order HBT coherence to study its properties via intensity interferometry with coincident two-photon photodetection. We introduce a momentum- and polarization-resolved

second-order HBT cross correlation, which probes both momentum and polarization entanglement and features quantum beats from the interference between the decay paths. The distinct pattern of polarization entanglement is a consequence of the axion coupling to the pseudoscalar Chern-Simons term.

An important corollary of hybridization is that a condensate of the cosmological axion, a main paradigm of theories of dark matter, induces a condensate of the synthetic axion, suggesting an indirect method of detecting the cosmological species from the excitation and decay of the condensed matter species, probed with HBT correlations.

The limit of vanishing coupling of the cosmological axion allows us to extend the results to the case of synthetic axions independently, since the two-photon final state features the kinematic and polarization entanglement properties as consequences of the Chern-Simons coupling to electromagnetic fields individually for each species. Therefore we argue that momentum- and polarization-resolved HBT second-order correlations are a useful probe to detect axionic collective excitations in condensed matter platforms. We point out a remarkable similarity to the phenomenon of parametric down conversion in nonlinear crystals, with correlations between the down-converted idler and signal photons that can be probed via HBT interferometry, thereby suggesting the same type of experimental setups to study axionic excitations in condensed matter systems.

In this theoretical study we did not address possible shortcomings and limitations arising from real materials and experimental realizations, nor have we discussed the various proposed materials as topological insulators or Weyl semimetals. We focused solely on the theoretical underpinnings of hybridization, its consequences such as quantum beats, and how to implement a possible theoretical framework to study them using intensity interferometry and HBT correlations. Obviously, the feasibility of observation of the phenomena associated with hybridization and or the implementation of interferometric studies of momentum and polarization entanglement with coincident two-photon photodetection and HBT correlations must be assessed experimentally.

A further avenue to study the correlations of the final two-photon state is to obtain the expectation value in this state of the quantum Stokes parameters introduced in Refs. [49–51]. In these references typically a monochromatic beam is assumed to propagate along a particular direction, and quantum Stokes parameters are associated with the perpendicular polarizations. This framework must be adapted to the case of the two-photon final state emerging from axion decay, because such a state is not monochromatic and is a mixture of polarizations. These aspects and their possible implementations as probes of axions will be the focus of further study.

ACKNOWLEDGMENTS

The author thanks Shuyang Cao for discussions during the early stages of this work, and gratefully acknowledges support from the U.S. National Science Foundation (NSF) through Grants No. NSF 2111743 and No. NSF 2412374.

DATA AVAILABILITY

No data were created or analyzed in this study.

APPENDIX A: HAMILTONIAN QUANTIZATION WITH A CHERN-SIMONS TERM

Let us consider the Lagrangian density of a generic pseudoscalar axion field $\phi(\vec{x},t)$ coupled solely to electromagnetism via a Chern-Simons term but in absence of external charge and current densities,

$$\mathcal{L}=\frac{1}{2}(\vec{E}^2(\vec{x},t)-\vec{B}^2(\vec{x},t))+g\phi(\vec{x},t)\,\vec{E}(\vec{x},t)\cdot\vec{B}(\vec{x},t)+\frac{1}{2}\left[\left(\frac{\partial}{\partial t}\phi(\vec{x},t)\right)^2-v^2\,(\vec{\nabla}\phi(\vec{x},t))^2-m^2\phi^2(\vec{x},t)\right], \tag{A1}$$

where v is a material dependent parameter in the case of synthetic axions and $v=1$ for the cosmological axion. In terms of the vector and scalar potentials $\vec{A}(\vec{x},t);A_0(\vec{x},t)$, respectively,

$$\vec{E}(\vec{x},t)=-\frac{\partial}{\partial t}\vec{A}(\vec{x},t)-\vec{\nabla}A_0(\vec{x},t),\quad \vec{B}(\vec{x},t)=\vec{\nabla}\times\vec{A}(\vec{x},t)\,. \tag{A2}$$

The equations of axion electrodynamics follow from the variational principle, these are given by [15]

$$\vec{\nabla}\times\vec{E}(\vec{x},t)=-\frac{\partial}{\partial t}\vec{B}(\vec{x},t)\,, \tag{A3}$$

$$\vec{\nabla}\cdot\vec{B}(\vec{x},t)=0\,, \tag{A4}$$

$$\vec{\nabla}\cdot\vec{E}(\vec{x},t)=-g\vec{B}(\vec{x},t)\cdot\vec{\nabla}\phi(\vec{x},t)\,, \tag{A5}$$

$$\vec{\nabla}\times\vec{B}(\vec{x},t)=\frac{\partial}{\partial t}\vec{E}(\vec{x},t)+g\left(\vec{B}(\vec{x},t)\,\frac{\partial}{\partial t}\phi(\vec{x},t)+(\vec{\nabla}\phi(\vec{x},t))\times\vec{E}(\vec{x},t)\right), \tag{A6}$$

and the equation of motion for the pseudoscalar field is

$$\frac{\partial^2}{\partial t^2}\phi(\vec{x},t)-v^2\nabla^2\phi(\vec{x},t)+m^2\phi(\vec{x},t)-g\vec{E}(\vec{x},t)\cdot\vec{B}(\vec{x},t)=0\,. \tag{A7}$$

Including external charge and current densities modify the right-hand side of Eqs. (A5), (A6) by the usual source terms in electrodynamics. In passing to the Hamiltonian description one recognizes that the coupling via the Chern-Simons term modifies the canonical momentum conjugate to $\vec{A}(\vec{x},t)$, whereas, as usual the canonical momentum conjugate to $A_0(\vec{x},t)$ vanishes,

$$\vec{\Pi}(\vec{x},t)=\frac{\partial\mathcal{L}}{\partial\dot{\vec{A}}(\vec{x},t)}=-\vec{E}(\vec{x},t)-g\,\phi(\vec{x},t)\,\vec{B}(\vec{x},t),$$
$$\Pi_0(\vec{x},t)=\frac{\partial\mathcal{L}}{\partial\dot{A}_0(\vec{x},t)}=0\,, \tag{A8}$$

and for the pseudoscalar field

$$\pi_\phi(\vec{x},t) = \frac{\partial}{\partial t}\phi(\vec{x},t)\,. \tag{A9}$$

We note that Eq. (A5) is not an equation of motion, as there are no time derivatives, but a constraint. In particular it yields the following constraint on the canonical momentum conjugate to the vector potential (in absence of external sources)

$$\vec{\nabla}\cdot\vec{\Pi}(\vec{x},t) = 0\,. \tag{A10}$$

The Hamiltonian density is obtained as usual

$$\mathcal{H} = \vec{\Pi}\cdot\frac{\partial}{\partial t}\vec{A} + \pi_\phi\frac{\partial}{\partial t}\phi - \mathcal{L} \tag{A11}$$

by expressing $\dot{\vec{A}}, \dot{\phi}$ in terms of $\vec{\Pi}, \pi_\phi$, respectively, yielding the total Hamiltonian

$$H = \int d^3x\Big\{\frac{1}{2}\vec{\Pi}^2 + \frac{1}{2}\vec{B}^2 - \vec{\Pi}\cdot\vec{\nabla}A_0 + g\phi\,\vec{\Pi}\cdot\vec{B} + \frac{g^2}{2}\phi^2\,\vec{B}^2 + \frac{1}{2}\pi_\phi^2 + \frac{v^2}{2}(\vec{\nabla}\phi)^2 + \frac{m^2}{2}\phi^2\Big\}\,. \tag{A12}$$

Hamilton's equations of motion yield

$$\dot{\vec{A}} = \vec{\Pi} - \vec{\nabla}A_0 + g\phi\vec{B}\,, \tag{A13}$$

$$\dot{\phi} = \pi_\phi\,, \tag{A14}$$

which are precisely the definition of the canonical momenta $\vec{\Pi}, \pi_\phi$, Eqs. (A8), (A9), respectively, and

$$\dot{\vec{\Pi}} = -(\vec{\nabla}\times\vec{B}) - g^2\{2\phi\,(\vec{\nabla}\phi\times\vec{B}) + \phi^2\,(\vec{\nabla}\times\vec{B})\} - g\{(\vec{\nabla}\phi\times\vec{\Pi}) + \phi(\vec{\nabla}\times\vec{\Pi})\}\,, \tag{A15}$$

$$\dot{\pi}_\phi = v^2\nabla^2\phi - m^2\phi - g\vec{\Pi}\cdot\vec{B} - g^2\phi\vec{B}^2\,. \tag{A16}$$

Using the first relation in Eq. (A8), the equations of motion (A6), (A7) are obtained after straightforward algebra. The equation (A10) cannot be obtained from Hamilton's equations of motion as it is a constraint. Using canonical commutation relations, it follows that $\vec{\nabla}\cdot\vec{\Pi}$ is the generator of time independent U(1) gauge transformations, just as $\vec{\nabla}\cdot\vec{E}$ in quantum electrodynamics (QED) without sources, therefore gauge invariant states are annihilated by $\vec{\nabla}\cdot\Pi$. Therefore, $\vec{\nabla}\cdot\vec{\Pi} = 0$ is a constraint that must be applied onto physical states, just as $\vec{\nabla}\cdot\vec{E} = 0$ in quantum electrodynamics without sources. Upon integration by parts in (A12) and using the constraint (A10), when acting on physical states, namely those annihilated by this constraint, the third term in the total Hamiltonian (A12) vanishes. It is convenient to work in Coulomb gauge

$$\vec{\nabla}\cdot\vec{A}(\vec{x},t) = 0\,, \tag{A17}$$

wherein the constraint (A10) becomes Poisson's equation with a source determined by the Chern-Simons term, namely

$$\nabla^2 A_0(\vec{x},t) = g\vec{B}(\vec{x},t)\cdot\vec{\nabla}\phi(\vec{x},t)\,. \tag{A18}$$

Adapting the Hamiltonian framework to the case of synthetic and cosmological axions, it is simply a matter of replacing

$$g\phi \to (g_s\phi_s + g_c\phi_c)\,, \tag{A19}$$

in the above results.

Interaction picture quantization

Upon integration by parts of the third term in (A12) and in the physical (gauge invariant) sector, imposing the constraint (A10), we write the Hamiltonian (A12) as

$$H = H_0 + H_I, \tag{A20}$$

where

$$H_0 = \int d^3x\Big\{\frac{1}{2}\vec{\Pi}^2 + \frac{1}{2}\vec{B}^2 + \frac{1}{2}\pi_\phi^2 + \frac{v^2}{2}(\vec{\nabla}\phi)^2 + \frac{m^2}{2}\phi^2\Big\} \tag{A21}$$

$$H_I = \int d^3x\Big\{g\phi\,\vec{\Pi}\cdot\vec{B} + \frac{g^2}{2}\phi^2\,\vec{B}^2\Big\}\,. \tag{A22}$$

Passing to the interaction picture of the free field Hamiltonian H_0,

$$H_I(t) = e^{iH_0t}H_Ie^{-iH_0t}\,. \tag{A23}$$

In interaction picture it follows that

$$\vec{\Pi}(\vec{x},t) = \dot{\vec{A}}(\vec{x},t), \quad \pi_\phi(\vec{x},t) = \dot{\phi}(\vec{x},t)\,, \tag{A24}$$

and the constraint (A10) is automatically fulfilled in Coulomb gauge (A17). In the interaction picture the quantization of the (pseudo)scalar degrees of freedom, namely synthetic (s) and cosmological (c) axions is achieved via the expansion in the quantization volume V

$$\phi_{s,c}(\vec{x},t) = \frac{1}{\sqrt{V}}\sum_{\vec{k}}\frac{1}{\sqrt{2E_{s,c}(k)}} \times\Big[b_{s,c}(\vec{k})\,e^{-iE_{s,c}(k)t}\,e^{i\vec{k}\cdot\vec{x}} + b^\dagger_{s,c}(\vec{k})\,e^{iE_{s,c}(k)t}\,e^{-i\vec{k}\cdot\vec{x}}\Big]\,, \tag{A25}$$

in Coulomb gauge, the vector potential is given by

$$\vec{A}(\vec{x},t) = \frac{1}{\sqrt{V}}\sum_{\vec{k}}\sum_{\lambda=1,2}\frac{\vec{\epsilon}_\lambda(\vec{k})}{\sqrt{2k}} \times\Big[a_\lambda(\vec{k})\,e^{-ikt}\,e^{i\vec{k}\cdot\vec{x}} + a^\dagger_\lambda(\vec{k})\,e^{ikt}\,e^{-i\vec{k}\cdot\vec{x}}\Big]\,, \tag{A26}$$

where the polarization unit vectors $\vec{\epsilon}_\lambda(\vec{k})$ are chosen real and $\hat{\vec{k}}, \vec{\epsilon}_{1,2}(\vec{k})$ form a right-handed triad with the properties

$$\vec{\epsilon}_1(\vec{k})\times\vec{\epsilon}_2(\vec{k}) = \hat{\vec{k}}, \quad \vec{\epsilon}_2(\vec{k})\times\hat{\vec{k}} = \vec{\epsilon}_1(\vec{k}), \quad \vec{\epsilon}_1(\vec{k})\times\hat{\vec{k}} = -\vec{\epsilon}_2(\vec{k}), \quad \vec{\epsilon}_1(-\vec{k}) = -\vec{\epsilon}_1(\vec{k}), \quad \vec{\epsilon}_2(-\vec{k}) = \vec{\epsilon}_2(\vec{k})\,. \tag{A27}$$

The annihilation and creation operators obey the usual canonical commutation relations. The magnetic field is as usual

$$\vec{B}(\vec{x},t) = \vec{\nabla} \times \vec{A}(\vec{x},t)\,, \tag{A28}$$

and the canonical momentum conjugate to the vector potential in Coulomb gauge and interaction picture is

$$\vec{\Pi}(\vec{x},t) = \frac{\partial}{\partial t}\vec{A}(\vec{x},t) = -\vec{E}(\vec{x},t)\,, \tag{A29}$$

We recognize that the last term in (A22) features ultraviolet divergences. The vacuum expectation value of the operator $\vec{B}^2$ features zero point divergences, which entail an ultraviolet divergent renormalization of the mass of the pseudoscalar field, and the vacuum expectation value of the operator ϕ^2 also features zero point ultraviolet divergences which entail a divergent renormalization of the permeability of the vacuum. Hence, we define the normal ordered interaction in (A22) as

$$g^2\phi^2\vec{B}^2 \to g^2 :\phi^2::\vec{B}^2:\,, \tag{A30}$$

where the normal ordering prescription in the interaction picture, $:(\cdots):$ corresponds to arranging the annihilation operators always to the right of creation operators. However, we will obtain the transition matrix elements to *linear order* in g_s and g_c, therefore we will only keep the linear order interaction Hamiltonian, which in the interaction picture and to this order is given by

$$H_I(t) = -\int d^3x(g_s\phi_s(\vec{x},t) + g_c\phi_c(\vec{x},t))\vec{E}(\vec{x},t)\cdot\vec{B}(\vec{x},t)\,, \tag{A31}$$

with all operators being in the interaction picture, wherein $\vec{E}$ is given by Eq. (A29).

APPENDIX B: CALCULATION OF THE SPECTRAL DENSITY

Writing

$$\vec{k}\cdot\vec{k}_1 = kk_1\cos(\theta), \quad d^3k_1 = 2\pi\, k_1^2 dk_1 d(\cos(\theta)) \tag{B1}$$

and defining

$$q \equiv |\vec{k}-\vec{k}_1| = \sqrt{k^2+k_1^2-2kk_1\cos(\theta)} \tag{B2}$$

the spectral density (4.5) becomes

$$\rho_{ab}(k_0;k) = \frac{g_a g_b}{32\pi^2 k\sqrt{E_a(k)E_b(k)}}\int_0^\infty dk_1 \int_{q^-}^{q^+} \times\,[(q+k_1)^2-k^2]^2\,\delta(k_0-k_1-q)\,dq\,, \tag{B3}$$

where

$$q^+ = (k_1+k), \quad q^- = |k-k_1|\,, \tag{B4}$$

using the delta function constraint, yielding $q+k_1=k_0$ leads to

$$\rho_{ab}(k_0;k) = \frac{g_a g_b}{32\pi^2 k\sqrt{E_a(k)E_b(k)}}\left(k_0^2-k^2\right)^2\int_0^\infty dk_1 \times\int_{q^-}^{q^+}\delta(k_0-k_1-q)\,dq\,. \tag{B5}$$

The q integral is nonvanishing and equal to one if the conditions

$$k_0>0, \quad |k_1-k| \leqslant k_0-k_1 \leqslant k+k_1\,, \tag{B6}$$

are fulfilled. A graphical analysis shows that these conditions are fulfilled, for

$$k_0 > k, \quad k_- \leqslant k_1 \leqslant k_+ \tag{B7}$$

where

$$k_\pm = \tfrac{1}{2}(k_0 \pm k)\,, \tag{B8}$$

finally yielding the result (4.6).

APPENDIX C: FIRST-ORDER CROSS CORRELATION

The calculation of the first-order cross correlation (4.23) is lengthy but straightforward, the result is the following:

$$\widetilde{G}^{(1)}(\vec{p}_1,s_1;\vec{p}_2,s_2;t) = \sum_{\lambda_2} C^*_{2\gamma}(\vec{p}_1,s_1;\vec{k}_2,\lambda_2;t)C_{2\gamma}(\vec{p}_1,s_2;\vec{k}_2,\lambda_2;t)\,\delta_{\vec{k}_2,\vec{k}-\vec{p}_1}\delta_{\vec{p}_1,\vec{p}_2} + \sum_{\lambda_1} C^*_{2\gamma}(\vec{p}_1,s_1;\vec{k}_1,\lambda_1;t)C_{2\gamma} \times(\vec{k}_1,\lambda_1;\vec{p}_1,s_2;t)\,\delta_{\vec{k}_1,\vec{k}-\vec{p}_1}\delta_{\vec{p}_1,\vec{p}_2} + \sum_{\lambda_2} C^*_{2\gamma}(\vec{k}_2,\lambda_2;\vec{p}_1,s_1;t)C_{2\gamma}(\vec{p}_1,s_2;\vec{k}_2,\lambda_2;t)\,\delta_{\vec{k}_2,\vec{k}-\vec{p}_1}\delta_{\vec{p}_1,\vec{p}_2} + \sum_{\lambda_1} C^*_{2\gamma}(\vec{k}_1,\lambda_1;\vec{p}_1,s_1;t)C_{2\gamma}(\vec{k}_1,\lambda_1;\vec{p}_1,s_2;t)\,\delta_{\vec{k}_1,\vec{k}-\vec{p}_1}\delta_{\vec{p}_1,\vec{p}_2} \tag{C1}$$

[1] R. D. Peccei and H. R. Quinn, CP conservation in the presence of pseudoparticles, Phys. Rev. Lett. **38**, 1440 (1977); Constraints imposed by CP conservation in the presence of pseudoparticles, Phys. Rev. D **16**, 1791 (1977).

[2] S. Weinberg, A new light Boson? Phys. Rev. Lett. **40**, 223 (1978).

[3] F. Wilczek, Problem of strong P and T invariance in the presence of instantons, Phys. Rev. Lett. **40**, 279 (1978).

[4] J. Preskill, M. B. Wise, and F. Wilczek, Cosmology of the invisible axion, Phys. Lett. B **120**, 127 (1983).

[5] L. F. Abbott and P. Sikivie, A cosmological bound on the invisible axion, Phys. Lett. B **120**, 133 (1983).

[6] M. Dine and W. Fischler, The not-so-harmless axion, Phys. Lett. B **120**, 137 (1983).

[7] T. Banks and M. Dine, Couplings and scales in strongly coupled heterotic string theory, Nucl. Phys. B **479**, 173 (1996).

[8] A. Ringwald, Exploring the role of axions and other WISPs in the dark universe, Phys. Dark Universe **1**, 116 (2012).

[9] D. J. E. Marsh, Axion cosmology, Phys. Rep. **643**, 1 (2016); F. Chadha-Day, J. Ellis, and D. J. E. Marsh, arXiv:2105.01406.

[10] P. Sikivie, Invisible axion search methods, Rev. Mod. Phys. **93**, 015004 (2021).

[11] CAST Collaboration, New CAST limit on the axion-photon interaction, Nature Phys. **13**, 584 (2017).

[12] ADMX Collaboration, Search for "invisible" axion dark matter in the 3.3 μeV mass range, Phys. Rev. Lett. **127**, 261803 (2021).

[13] P. W. Graham, I. G. Irastorza, S. K. Lamoreaux, A. Lindner, and K. A. van Bibber, Experimental searches for the axion and axion-like particles, Annu. Rev. Nucl. Part. Sci. **65**, 485 (2015).

[14] I. G. Irastorza and J. Redondo, New experimental approaches in the search for axion-like particles, Prog. Part. Nucl. Phys. **102**, 89 (2018).

[15] F. Wilczek, Two applications of axion electrodynamics, Phys. Rev. Lett. **58**, 1799 (1987).

[16] X.-L. Qi, T. L. Hughes, and S.-C. Zhang, Topological field theory of time-reversal invariant insulators, Phys. Rev. B **78**, 195424 (2008).

[17] A. Sekine and K. Nomura, Axion electrodynamics in topological materials, J. Appl. Phys. **129**, 141101 (2021).

[18] R. Li, J. Wang, X.-L. Qi, and S.-C. Zhang, Dynamical axion field in topological magnetic insulators, Nature Phys. **6**, 284 (2010).

[19] J. Wang, B. Lian, and S.-C. Zhang, Dynamical axion field in a magnetic topological insulator superlattice, Phys. Rev. B **93**, 045115 (2016).

[20] D. M. Nenno, C. A. C. Garcia, J. Gooth, C. Felser, and P. Narang, Axion physics in condensed-matter systems, Nature Rev. Phys. **2**, 682 (2020).

[21] J. Gooth, B. Bradlyn, S. Honnali, C. Schindler, N. Kumar, J. Noky, Y. Qi, C. Shekhar, Y. Sun, Z. Wang, B. A. Bernevig, and C. Felser, Axionic charge-density wave in the Weyl semimetal $(TaSe_4)_2I$, Nature (London) **575**, 315 (2019).

[22] J. Yu, B. J. Wieder, and C.-X. Liu, Dynamical piezomagnetic effect in time-reversal-invariant Weyl semimetals with axionic charge density waves, Phys. Rev. B **104**, 174406 (2021).

[23] E. Mottola, A. V. Sadofyev, and A. Stergiou, Axions and superfluidity in Weyl semimetals, Phys. Rev. B **109**, 134512 (2024).

[24] L. Shaposhnikov, M. Mazanov, D. A. Bobylev, F. Wilczek, and M. A. Gorlach, Emergent axion response in multilayered metamaterials, Phys. Rev. B **108**, 115101 (2023).

[25] L. Wu, M. Salehi, N. Koirala, J. Moon, S. Oh, and N. P. Armitage, Quantized Faraday and Kerr rotation and axion electrodynamics of a 3D topological insulator, Science **354**, 1124 (2016).

[26] W. K. Tse and A. H. MacDonald, Giant magneto-optical kerr effect and universal faraday effect in thin-film topological insulators, Phys. Rev. Lett. **105**, 057401 (2010).

[27] J. Ahn, S.-Y. Xu, and A. Vishwanath, Theory of optical axion electrodynamics and application to the Kerr effect in topological antiferromagnets, Nature Commun. **13**, 7615 (2022).

[28] K. Ishiwata and K. Nomura, Collective excitations in magnetic topological insulators and axion dark matter search, J. High Energy Phys. 10 (2024) 225.

[29] Z.-Q. Gao, T. Wang, M. P. Zaletel, and D.-H. Lee, Detecting axion dynamics on the surface of magnetic topological insulators, arXiv:2409.17230.

[30] D. J. E. Marsh, K.-C. Fong, E. W. Lentz, L. Šmejkal, and M. N. Ali, Proposal to detect dark matter using axionic topological antiferromagnets, Phys. Rev. Lett. **123**, 121601 (2019).

[31] J. Schütte-Engel, D. J. E. Marsh, A. J. Millar, A. Sekine, F. Chadha-Day, S. Hoof, M. Ali, K.-C. Fong, E. Hardy, and L. Šmejkal, Axion quasiparticles for axion dark matter detection, J. Cosmol. Astropart. Phys. 08 (2021) 066.

[32] S. Chigusa, T. Moroi, and K. Nakayama, Axion/hidden-photon dark matter conversion into condensed matter axion, J. High Energy Phys. 08 (2021) 074.

[33] M. O. Scully and M. S. Zubairy, *Quantum Optics* (Cambridge University Press, Cambridge, 1997).

[34] P. Meystre and M. Sargent III, *Elements of Quantum Optics*, 4th ed. (Springer, New York, 2007).

[35] B. M. Garraway and P. L. Knight, Cavity modified quantum beats, Phys. Rev. A **54**, 3592 (1996).

[36] G. C. Hegerfeldt and M. B. Plenio, Quantum beats revisited: A quantum jump approach, Quantum Opt. **6**, 15 (1994).

[37] V. Weisskopf and E. Wigner, Calculation of the natural brightness of spectral lines on the basis of Dirac's theory, Z. Phys. **63**, 54 (1930).

[38] S. Cao and D. Boyanovsky, Brownian axionlike particles, Phys. Rev. D **106**, 123503 (2022); Nonequilibrium dynamics of axionlike particles: The quantum master equation, *ibid.* **107**, 063518 (2023).

[39] R. J. Glauber, Optical coherence and photon statistics, in *Quantum Optics and Electronics*, edited by B. De Witt, C. Blandin, and A. Cohen-Tannoudji, Vol. 63 (Gordon and Breach, New York, 1965), pp. 65–185; R. J. Optical, Photon correlations, Phys. Rev. Lett. **10**, 84 (1963).

[40] R. H. Brown and R. Q. Twiss, Correlation between photons in two coherent beams of light, Nature (London) **177**, 27 (1956); A test of a new type of stellar interferometer on Sirius, **178**, 1046 (1956); Interferometry of the intensity fluctuations in light-I. Basic theory: The correlation between photons in coherent beams of radiation, Proc. Roy. Soc. A **242**, 300 (1957).

[41] L. Mandel and E. Wolf, *Optical Coherence and Quantum Optics*, (Cambridge University Press, Cambridge, 1995).

[42] B. Silva, C. Sánchez Muñoz, D. Ballarini, A. González-Tudela, M. de Giorgi, G. Gigli, K. West, L. Pfeiffer, E. del Valle, D. Sanvitto, and F. P. Laussy, The colored Hanbury Brown–twiss effect, Sci. Rep. **6**, 37980 (2016).

[43] M. Scully, Photon-Photon correlations from single atoms, in *Advances in Quantum Phenomena*, edited by E. G. Beltrametti and J. M. Levy-Leblond, (Plenum Press, New York, 1995), p. 335.

[44] O. Liebman, J. Curtis, I. Petrides, and P. Narang, Multiphoton spectroscopy of a dynamical axion insulator, arXiv:2306.00064.

[45] R. Ghosh, C. K. Hong, Z. Y. Ou, and L. Mandel, Interference of two photons in parametric down conversion, Phys. Rev. A **34**, 3962 (1986).

[46] C. K. Hong, Z. Y. Ou, and L. Mandel, Measurement of subpicosecond time intervals between two photons by interference, Phys. Rev. Lett. **59**, 2044 (1987).

[47] M. H. Rubin, D. N. Klyshko, Y. H. Shih, and A. V. Sergienko, Theory of two-photon entanglement in type-II optical parametric down-conversion, Phys. Rev. A **50**, 5122 (1994).

[48] Z. Y. Ou and L. Mandel, Violation of Bell's inequality and classical probability in a two-photon correlation experiment, Phys. Rev. Lett. **61**, 50 (1988); Y. H. Shih and C. O. Alley, New type of einstein-podolsky-rosen-bohm experiment using pairs of light quanta produced by optical parametric down conversion, *ibid.* **61**, 2921 (1988); T. E. Kiess, Y. H. Shih, A. V. Sergienko, and C. O. Alley, Einstein-Podolsky-Rosen-Bohm experiment using pairs of light quanta produced by type-II parametric down-conversion, *ibid.* **71**, 3893 (1993).

[49] D. Kuebel and T. D. Visser, Generalized Hanbury Brown-Twiss effect for stokes parameters, J. Opt. Soc. Am. A **36**, 362 (2019).

[50] X. Liu, G. Wu, X. Pang, D. Kuebel, and T. D. Visser, Polarization and coherence in the Hanbury Brown-Twiss effect, J. Mod. Opt. **65**, 1437 (2018).

[51] G. Björk, J. Soderholm, L. L. Sanchez-Soto, A. B. Klimov, J. Ghiu, P. Marian, and T. A. Marian, Quantum degrees of polarization, Opt. Commun. **283**, 4440 (2010).